Air and nutrient solution temperatures influence growth, development, mineral nutrients, and storage of five culinary herbs

A Thesis Presented for the

Master of Science

Degree

The University of Tennessee, Knoxville

Spencer R. Givens

May 2025

ABSTRACT

Culinary herbs are specialty crops commonly grown in controlled environment agriculture (CEA) using glass-glazed greenhouses. Greenhouses extend seasons and enhance environmental control but energy costs are prohibitive. Air temperature regulation during cold and hot seasons is particularly energy expensive. Air temperature effects on culinary herb growth, development, and tissue mineral concentrations are well-explored; however, rootzone temperature effects and interactions with air temperature are comparatively less characterized. Characterizing air and rootzone temperatures' interactions could assist hydroponic producers they could regulate rootzone temperature and reduce air temperature control to increase efficiency and potentially improve yield and quality. Therefore, the research objective was to [1] quantify the effects of, and interactions between, air and nutrient solution temperatures on growth, development, shoot tissue mineral concentrations, and postharvest storage of four culinary herb species. To achieve those objectives, we grew basil (*Ocimum basilicum*) 'Nufar' and 'Red Rubin', cilantro (*Coriandrum sativum*) 'Santo', common sage (*Salvia officinalis*), and parsley (*Petroselenium crispum*) 'Giant of Italy' in deep-water-culture tanks with 15, 20, 25, 30, or 35 ° [degrees] C nutrient solution temperatures with 20 or 30 ° [degrees] C air temperature. At harvest, we quantified plant yield, development, and mineral concentrations, and stored fresh tissue in coolers held at 4 and 10 ° [degrees] C for 12 days. Basil 'Nufar' and 'Red Rubin' yielded the greatest fresh mass, dry mass, nodes and longest stems in 25-30 ° [degrees] C nutrient solution temperature with 30 ° [degrees] C air temperature. Basil grown in high air and nutrient solution temperatures greater than or equal to 30 ° [degrees] C lost water at a reduced rate compared to those grown in lower temperatures. Cilantro 'Santo' fresh mass, dry mass, and leaf number were not significantly influenced by air temperature, but quadratically increased as nutrient solution temperature increased from 15 to 25 ° [degrees] C. Common sage and parsley 'Giant of Italy' fresh mass, height, and leaf and node numbers were greatest in 25 ° [degrees] C nutrient solution. Producers may regulate nutrient solutions to achieve temperatures of 25 to 30 ° [degrees] C for adequate shelf life and biomass yield.

TABLE OF CONTENTS

Chapter I: Literature Review……..……...…...1

Controlled environment agriculture…….....……..2

Greenhouse temperature control……...……...…..3

Plant responses to temperature……..…….....7

Culinary herb production……..……...….11

Chapter II: Air and nutrient solution temperature affect the growth, development, and mineral nutrition of five culinary herbs……...……..14

Abstract……..……..…….15

Introduction……..……17

Materials and methods…….……...17

Plant Production…….....17

Environmental Conditions…….……18

Data Collection……..19

Mineral Analyses……...20

Experimental Design and Statistical Analyses……..22

Results……...23

Basil'Nufar'…….……..28

Basil 'Red Rubin'……...……30

Cilantro 'Santo'…….36

Common Sage……43

Parsley 'Giant of Italy'……..43

Discussion……...……..43

Conclusion…….……...……49

Chapter III: Air and nutrient solution temperature influence basil postharvest weight loss…….51

Abstract……...…….52

Introduction…….....52

Materials and methods……....53

Growing conditions……53

Data collection……...53

Experimental design and data analysis……..…54
Results …….…….....55
Basil 'Nufar'……..55
Basil 'Red Rubin'……...…55
Discussion …...…….59
Conclusion……...…….60
Literature cited ……..……..……..61
Vita……76

LIST OF TABLES

Table 1. Average daily air temperature, nutrient solution temperature, relative humidity, and daily light integral (± standard error of the mean) are displayed for basil (Ocimum basilicum) 'Nufar' and 'Red Rubin', cilantro (Coriandrum sativum) 'Santo', parsley (Petroselenium crispum) 'Giant of Italy', and common sage (Salvia officinalis). [X]RH= Relative Humidity, [Y]DLI = daily light integral, [Z]Dash lines = no data, *missing data.…….....20

Table 2. Linear, quadratic, and surface regression coefficients for basil (*Ocimum basilicum*) 'Nufar' and 'Red Rubin', cilantro (*Coriandrum sativum*) 'Santo', parsley (*Petroselenium crispum*) 'Giant of Italy', and common sage (*Salvia officinalis*) growth and development responses to air and nutrient solution temperatures. Letters as superscripts designate the following: [Z]Coefficients for model equations; [Y]Dash lines = 0; [X]Standard error of the mean; [W] Fresh mass; [V]Shoot dry mass; [U]Leaf dry mass; [T]Stem dry mass; [S]PH = Plant height, SL = Shoot length; [R]Internode length; [Q]Leaf to stem ratio; [P]Node number; [O]Dry matter concentration. Statistical model: $\{f(x) = y0 + a \cdot x + b \cdot y + c \cdot x^2 + d \cdot y^2 + e \cdot x \cdot y\}$ [x = AT °C] [y = NST °C]……...…….....24

Table 3. Linear, quadratic, and surface regression coefficients for basil 'Nufar' and 'Red Rubin', cilantro 'Santo' dry shoot concentrations responses to air and nutrient solution temperatures. Letters as superscripts designate the following: [Z]Coefficients for model equations used to generate Figs. 1, 4, 7, 11, and 12; [Y]Dash lines = 0; [X]Carbon; [W]Nitrogen; [V]Phosphorus; [U]Potassium; [T]Calcium; [S]Magnesium; [R]Sulfur; [Q]Boron; [P]Copper; [O]Iron; [N]Manganese; [M]Molybdenum; and [L]Zinc. Statistical model: $\{f(x) = y0 + a \cdot x + b \cdot y + c \cdot x^2 + d \cdot y^2 + e \cdot x \cdot y\}$ [x = AT °C] [y = NST °C]….....……..26

Table 4. Basil 'Nufar' and 'Red Rubin' weight loss ([Z]) (% w/w) during storage. [Y]Model terms corresponding to linear mixed effect model on page 53 and [X]ns = response was not statistically significant. …….56

LIST OF FIGURES

Figure 1. Basil (*Ocimum basilicum*) 'Nufar' air temperature and nutrient solution temperature interaction effects on fresh mass (A), shoot dry mass (B), node number (C), leaf dry mass (D), stem dry mass (E), leaf to stem ratio (F; axes are transposed), plant height (G), and internode length (H), air temperature influence on dry matter concentration (I), and nutrient solution temperature influence on dry matter concentration (J). ……...29

Figure 2. Basil (*Ocimum basilicum*) 'Nufar air temperature and nutrient solution temperature interaction effects on dry shoot concentrations (percent dry mass or $\mu g \cdot g^{-1}$) of phosphorus (A), calcium (B), magnesium (C), sulfur (D), copper (E), manganese (F), and molybdenum (G) 31

Figure 3. Air temperature influences on basil (*Ocimum basilicum*) 'Nufar' dry shoot concentrations (%w/w) of nitrogen (A) and potassium (B), as well as nutrient solution temperature influences on nitrogen (C), potassium (D), iron (E), and zinc (F) concentrations……32

Figure 4. Basil (*Ocimum basilicum*) 'Red Rubin' air temperature and nutrient solution temperature interaction effects on fresh mass (A), shoot dry mass (B), plant height (C), leaf dry mass (D), stem dry mass (E), internode length (F), air temperature influence on node number (G), leaf to stem ratio (H), dry matter concentration (I), and nutrient solution temperature influence on node number (J) and dry matter concentration (K) ……..33

Figure 5. Basil (*Ocimum basilicum*) 'Red Rubin' air temperature and nutrient solution temperature interaction effects on shoot concentrations of calcium (A), magnesium (B), iron (C), boron (D), and molybdenum (E)…….…….....35

Figure 6. Air temperature effects on basil (*Ocimum basilicum*) 'Red Rubin' dry shoot concentrations of potassium (A), sulfur (C), copper (E), manganese (G), zinc (I), and phosphorus (K); as well as nutrient solution temperature effects on potassium (B), sulfur (D), copper (F), manganese (H), zinc (J), and nitrogen (L) ……37

Figure 7. Air and nutrient solution temperature interaction effects on cilantro (*Coriandrum sativum*) 'Santo' dry matter concentration (A) and plant length (B), air temperature effects on leaf number (F), and nutrient solution temperature effects on shoot dry mass (C), fresh mass (D), and leaf number (E) …….…….38

Figure 8. Air and nutrient solution temperature interaction effects on cilantro (*Coriandrum sativum*) 'Santo' shoot concentrations of potassium (A) and copper (B) …….……40

Figure 9. Air temperature effects on cilantro (*Coriandrum sativum*) ‘Santo’ dry shoot concentrations of nitrogen (A), phosphorus (C), sulfur (E), boron (G), iron (I); as well as nutrient solution temperature effects on nitrogen (B), phosphorus (D), sulfur (F), boron (H), iron (J), calcium (K), magnesium (L), and molybdenum (M) 41
Figure 10. Air temperature influence on cilantro (*Coriandrum sativum*) ‘Santo’ manganese (A) and zinc (B), as well as nutrient solution temperature influence on manganese (C) and zinc (D)……..42
Figure 11. Nutrient solution temperature effects on common sage (*Salvia officinalis*) fresh mass (A), plant length (B), and node number (C) ……..…….……...44
Figure 12. Nutrient solution temperature effects on parsley (*Petroselenium crispum*) ‘Giant of Italy’ fresh mass (A), plant height (B), and leaf number (C) ...…….……45
Figure 13. Air and nutrient solution temperature effects on weight loss during storage of basil (*Ocimum basilicum*) ‘Nufar’, over 4 to 12 days in storage in 4 or 10 °C ...……..57
Figure 14. Air and nutrient solution temperature effects on weight loss during storage of basil (*Ocimum basilicum*) ‘Red Rubin’ over 6, 10, and 12 days in storage ...…….…..58

Chapter I

Literature Review

Controlled environment agriculture

Controlled environment agriculture (CEA) is an established and growing sector of food and specialty crop production. The goal of CEA is to maintain growing conditions actively or passively, which improves consistency, quality, and yield. Greenhouses, indoor growth chambers, and hoop houses are a few forms of CEA. Climate models suggest that anthropogenic forcings could destabilize our agricultural systems and directly damage field crop yields due to heat stresses, extreme weather events, and disrupted hydrologic cycles (Asseng, 2015; Christensen and Christensen, 2007; Hatfield, 2011; Slattery and Ort, 2019). Thus, CEA could partially insulate our food supply chains from climatic instability, by securing high yields in maintained conditions. Controlled environment production can prove effective in localities which have limited supplies of freshwater and arable land, or those with short growing seasons, but production is growing rapidly across the United States (US) and especially in areas with advantageous climates for production such as California (Steward and Avery, 2022).

Local producers in urban and suburban areas must contend with the cost of scarce and expensive land, thus commercial CEA production in the US is concentrated in localities which have suitable climates and ample arable land area (Gasperi et al., 2017). Produce crops require shipping, handling, and processing to retain reasonable quality and shelf life at groceries (Martinez, 2010). The logistical expense of crop transport and potential for supply chain disruption may reduce produce availability in urban and suburban centers (Waliczek and Zajicek, 2016). Further, the cost and footprint of produce transport are predominantly determined by the distance between consumers and grocery stores; as a result, community-scale local production could reduce the carbon footprint and cost of locally grown produce, while also protecting produce access from supply chain shocks to long-distance transport (Mundler and Rumpus, 2012; Van Passel, 2021). Crop intensification through CEA could improve access to fresh produce; however, CEA often fails to cost-compete with field production, due in part to high capital and operating costs.

At present, CEA's market-share is expanding, but barriers to growth remain in place. High energy use significantly limits CEA's potential (Goldsten, 2016). Greenhouses are economical and popular because solar radiation is a cost-free source of light and heat. Glass panes are sturdy and provide high sunlight transmittance; consequently, most commercial greenhouses for food crops are glazed with glass (Nijskens, 1984). Despite the advantages of

glass, glass-glazed greenhouses suffer from conductive, infiltrative, and convective heat loss and gain, which reduces the energy-efficiency of air temperature control and raises production costs (Aguilar-Santana et al., 2020; Runkle and Both, 2011). Solar radiation provides free light as well as heat gain (Li, 2019). Solar heat gain, in simplified form, proceeds as follows: sunlight is transmitted through the glazing, then gets absorbed by interior surfaces and re-emitted as infrared radiation which is partially "trapped" in the greenhouse (Al-Mahdouri et al., 2013; Bredenbeck, 1984).

Greenhouse Temperature Control

To achieve optimal conditions for crop production, producers passively or actively regulate greenhouse air temperature (AT). Semi-passive methods minimize heat loss or gain with minimal energy use, while active methods require consistent energy input. Commercial greenhouses often utilize a combination of semi-passive and active temperature controls to enhance their energy-use-efficiency. Further, semi-passive methods have longer response times and lower total cooling or heating capacity compared with active methods (Lorenzo et al., 2021). Therefore, a combined approach employs passive strategies to maintain a baseline level of cooling or heating, to increase the efficiency of active strategies, and to reduce energy use; on the other hand, active strategies fulfill excess, sudden demand, though at greater cost.

Semi-passive cooling methods include shade cloth, ultraviolet (UV) and/or infrared (IR) resistant coatings, and reflective paint, while active cooling employs fans, vents, mobile shade curtains, and evaporative pad or mist systems (Choab et al., 2019). Shade cloth, UV or IR reflective coatings, and reflective paint minimize solar gain by reflecting light off greenhouse surfaces or filtering out only certain wavelengths (IR or UV range) of light (Ahemd, 2016). Shading is highly effective during peak sunlight hours and can lower greenhouse temperatures by up to 10 °C, but it lowers available light to plants, and the cloth must be periodically replaced to ensure even and effective light distribution (Ahemd et al., 2016; Papadakis et al., 2000). Cloth or reflective film shade systems are either fixed in place or retractable. Retractable shade systems pull cloth or reflective film along tracks situated above the production area, to achieve a coverage area which is determined by feedback from air temperature sensors. Retractable shading is customizable, and therefore more flexible relative to fixed systems, but it requires specialized motors, tracks, and maintenance, and thus it is more costly (Kittas et al., 2005). Ventilation is a key aspect of greenhouse temperature regulation and consists of forced air and

passive systems. Passive ventilation consists of roof and/or sidewall-mounted vents, which are controlled mechanically or by hand and provide an entryway or exit for outside air. Rooftop vents may "purge" excess humidity and heat, which accumulate towards the peak of the greenhouse roof. Side or end-wall fans are essential components of forced ventilation systems and increase air exchanges with the outside. Forced ventilation lowers vapor pressure, mixes air to ensure even temperatures, and reduces relative humidity inside the greenhouse (Willits, 2003). Pad or mist systems disperse water over a porous medium, or throughout large volumes of air; after dispersal, the water draws heat from the air as it evaporates, thus the air temperature within the greenhouse cools (Sethi, 2007). Evaporative cooling can reduce greenhouse temperatures by 2 to 12 °C, depending on the system and environmental conditions (Misra and Gosh, 2018). Humid climates with low vapor pressure deficits reduce the efficiency of evaporative cooling, as the water in those systems evaporates slower and thus exchanges less heat with the air. Likewise, pumps and fans experience greater mechanical wear and energy demands under constant use when compared with intermittent use.

Producers heat greenhouses with semi-passive methods, such as solar gain, thermal curtains, and phase change materials; and active methods, such as radiative heaters, furnaces, steam, and hot-liquid-water (hydronic) systems (Li et al., 2019; Zhang et al., 2019). In many climates, solar gain fulfills greenhouse heat demands during daylight hours for much of the year, but cloud cover or long cold seasons can reduce its efficacy. Thermal curtains consist of insulating materials which are usually employed on fixed schedules during nighttime because ambient AT drops during the night and daytime use may cause excess shading. Passive heating generally cannot meet the demand of large commercial greenhouses, especially during cold seasons.

Steam, hydronic, and furnace systems require fuels such as natural gas, gasoline, coal, or wood; thus, active greenhouse heating can emit dangerous fumes including toxic, foul gases such as hydrogen sulfide, ozone, carbon monoxide, and ethylene if the source materials contain byproducts or incomplete combustion occurs (Chau et al., 2009; Hare, 1984). Toxic exhaust fumes necessitate filtration or ventilation systems, which can be costly, and ethylene emissions can modulate plant development and disrupt production timelines (Gibson et al., 2000). Ethylene is a plant hormone which can negatively impact crop production by inducing premature fruit ripening, flower bud abortion, and leaf senescence. To distribute heated air from furnaces or

radiators, producers employ horizontal air flow fans, occasionally with convection tubes, which are tubular plastic films with vent-holes cut at regular intervals, or through heating, ventilation, and air-conditioning (HVAC) ducts and out of metal vents situated in the production area (Bartok, 2001). Furnace or radiative air heaters are reasonably inexpensive and effective but suffer from inefficiency due to the lability of AT, large total air volumes, and losses from conduction and infiltration (Sethi et al., 2013). Steam or hydronic systems, on the other hand, circulate heated water through pipes placed in the production area (Sethi et al., 2013). Iron or aluminum pipes are required to distribute steam and hot liquid water due to the high operational temperatures and pressures, though lower temperature hydronic systems (≤32.2 °C) may use plastic pipes. Fins or ribs on the exterior surfaces of metal pipes maximize heat exchange with the air. To reduce heat waste, producers may opt to place rubber insulation sheaths around pipes in areas where heating is unneeded (Bartok, 2001). Perimeter heating pipes span the walls and/or ceilings of greenhouse bays; on the other hand, under-bench or root-zone heating pipes sit below benches, within the soil, substrate, or nutrient solution, or embedded within a concrete floor (Garcia et al., 1998).

Heat loss to the ambient environment, specialized labor for maintenance and construction, and high energy demands make active greenhouse heating expensive (Yildiz, 2021). In northern climates, environmental control systems must account for sunlight limitations, extreme cold, and snowpack on the greenhouse exterior during substantial parts of the year (Mcartney and Lefsrud, 2018). Greenhouse energy use is a dynamic function which depends upon the following: the climate control system, ambient climate, and construction; as well as crop needs, growth rates, and species/cultivars (Golzar et al., 2018). Thus, a “one size fits all” approach does not exist; however, to facilitate greater access to CEA, improve profits, and reduce resource use, we must develop temperature control strategies which maximize efficiency. One management practice which may improve yield and reduce energy cost is different temperature setpoints during day and night (DIF) (Elings et al., 2005).

Daytime AT in nature is usually warmer than nighttime AT due to solar irradiance (Balling and Cerveny, 2003; Sun et al., 2006). Greenhouse growers adjust temperature setpoints to resemble natural diurnal temperature ranges and reduce energy consumption (Sigrimis et al., 2000; Willits and Peet, 1998). Production DIF is the difference between average day and night temperatures.

In southern climates with warm summers, producers may maintain day temperatures which slightly exceed a crop's optimum temperature, if they cool aggressively during the night to reduce the average daily temperature (ADT) to the optimal range (Willits and Peet, 1998). A higher temperature setpoint during the day would allow the producers to expend less energy and place less wear on their cooling systems during peak surface insolation, while maintaining lower temperatures during the night is less expensive because solar gain becomes negligible. Aside from energy savings, a positive DIF setting may also alter plant quality, yield, and delay or enhance the transition between developmental stages for flowering crops (Bergstrand, 2015).

Optimal daytime production AT for most crops generally ranges from 1 to 10 °C higher than nighttime AT (DIF = 1-10) (Imler et al., 2020, 2022; Inthichack et al., 2013). Under dark conditions, plants mobilize photosynthates to maintain basic cellular functions; however, photosynthetic activity ceases. Thus, nocturnal photosynthate demands may produce an energy deficit (Hatfield et al., 2011). Under a positive DIF environments, the cooler nighttime temperatures reduce plants' nocturnal respiration rates, which could cut photosynthate loss.

Under-bench or direct root-zone heating localizes heat around the plant canopy and in the root-zone. Localized heat application minimizes waste compared to perimeter systems which heat a larger volume of air (Kawasaki et al., 2019; Kim et al., 2024). Direct root-zone heating is applicable to soil, substrate, or hydroponic production. Hydroponic production is especially attractive for root-zone temperature (RZT) control, due to the following: heat distributed throughout a body of liquid water is highly homogenous, it reduces the risk of drying out root-zones, and it minimizes thermal loss to the ambient environment and air (Rykbost, 1973). Root-zone temperature in hydroponic production is also called nutrient solution temperature (NST). Nutrient solution cooling during extreme summer heat could reduce costs associated with air-cooling, improve dissolved oxygen concentration, and avoid heat stress to plant roots (Moon et al., 2007). Likewise, producers could lower AT setpoints below the temperature optimum for a given plant if the NST heating could yield comparably to the AT optimum. Low-cost electric aquarium heaters and chillers, along with tank-type domestic water heaters, are all affordable options for small to medium scale producers; despite this, aquarium heaters and chillers are predominantly used on a hobby or research scale. Researchers have found improved biomass yield, produce quality, and nutritional value of lettuce (*Lactuca* spp.), cucumber (*Cucumis* spp.), spinach (*Spinacia oleracea*), tomato (*Solanum lycopersicum*), pepper (*Capsicum* spp.), eggplant

(*Solanum melongena*) and coriander (*Coriandrum sativum*) with nutrient solution heating in low air temperatures or cooling strategies in high air temperatures (Al-Rawahy et al., 2018; Chadirin et al., 2011; Hurewitz and Jane, 1983; Miller et al., 2020; Moon et al., 2007; Nkansah and Ito, 1994; Thompson et al., 1998). For instance, Miller et al. (2020) grew lettuce in heated and unheated nutrient solutions in low air temperature (13.7 °C) and found that heating the nutrient solutions improved shoot dry weight and water content compared to plants grown in unheated solutions.

Plant Responses to Temperature

Enzymes catalyze practically every chemical reaction which takes place in organisms, and they help to orient reagents, stabilize intermediate compounds, gate transport between cellular compartments, facilitate hormone signaling, and regulate gene transcription, translation, and expression (Copley, 2012). The temperature of the reaction environment determines substrate specificity and availability, molecule transport kinetics, conformation of enzymes' active sites, and allosteric regulation (Michaletz, 2015).

Plant metabolism is classified as primary or secondary. Primary metabolic processes are near ubiquitous among plant species and play necessary roles in plant growth and development. General primary metabolism pathways include cellular respiration and photosynthesis, lipid biosynthesis and partitioning, and hormone biosynthesis and signaling (Maeda, 2019). Primary metabolism directly influences growth metrics such as caliper and root ball size, biomass production, and node number, which dictate monetary value for some crops (Kläring et al., 2015). Metabolites such as sugars and lipids influence crop quality, shelf-stability, and overall hardiness. Sugars and lipids also buffer plant cells from osmotic stress, fuel adaptive responses to stressors, and promote strong development (Sanchez et al., 1998). Primary metabolism is foundational to all plant functions; on the other hand, secondary metabolism is more derived, and metabolites vary between species, cultivars, developmental stages, climates, and life histories (Esteban et al., 2009; Siegler et al., 1998).

Secondary metabolites constitute a diverse collection of compounds with "unessential" functions in plant growth and development, and some are unique to select species (Harborne, 1999; Pichersky, 2000, Siegler et al., 1998). Pigments and volatile organic compounds are two general categories of secondary metabolites (Alvarez, 2014). Pigments are colorant, structural, protective, and metabolic compounds in plants. Anthocyanins, for instance, are flavonoid

pigments which accumulate in epidermal cells and impart a red to black, often purplish, hue to plant tissue. Excess irradiance and cold temperatures can induce anthocyanin production in plant epidermal cells following a surge in reactive oxygen species (ROS) associated with those stresses, which anthocyanins may effectively scavenge (Naing et al., 2021; Zhu et al., 2018). Volatile organic compounds (VOCs) are secondary metabolites which defend plants, attract pollinators, and provide unique flavors and aromas (Obata, 2019). Secondary metabolism impacts plant nutritional value, appearance, flavor, and aroma, all of which are important to producers and consumers. Primary and secondary metabolism are influenced by ambient environmental conditions.

Plant species have colonized and evolved in virtually every climate upon nearly every continent, thus there are species and cultivar-specific optimal temperatures (T_o) for growth, development, and metabolite production (Gabor et al., 2017; Poelwijk et al., 2007; Xiaocheng et al., 2022). Aside from T_o, plant species' base temperatures (T_b) and maximum temperatures (T_m) are the lowest and highest temperatures at which a process may occur (Abrami, 1972). Specific T_b, $T_{o,\text{ and }}T_m$ values for a given species depend on the process, so temperature setpoint guidance for producers must account for the desired traits in the finished crop. Two-dimensional response curves represent plant thermal responses as a line, with temperature as the independent variable (x-axis) and the parameter of interest as the response, or dependent. variable (y-axis). A full-range response curve intercepts the x-axis at two points, once at T_b and once at T_m (Yan, 1999). The line peak represents T_o. The linear range, where the response variable increases linearly with temperature, lays between T_b and T_o (Luo, 2011). Temperatures beyond T_o begin to decrease the response trend, and the curve continues to drop until it reaches T_m. Plants grow in dynamic environments and require sufficient light, moderate temperature, oxygenated water, an atmosphere with carbon dioxide and oxygen, and essential mineral nutrients. Each environmental parameter a plant is subject to may interact with other environmental parameters, thus a given temperature response curve must be interpreted in context and is subject to variability (Dusenge et al., 2018). Regardless, low temperatures (LT) below T_b or high temperatures (HT) above T_m are usually deleterious; however, plants possess innate and adaptive mechanisms to protect themselves from thermal stress.

Basal thermal tolerance (BTT) and acquired or acclimated thermal tolerance (ATT) are two major categories of plant responses to thermal stressors (Hasanuzzaman, 2013). Basal

thermal tolerance is a plant's innate or baseline reaction to sudden or intense HT or LT exposure, without time for gradual acclimation. Plants are categorized as cold-tolerant ($T_b \leq 4$ °C), cold-temperate (4 °C < $T_b \leq 7$ °C), or cold-sensitive ($T_b > 7$ °C) (Lopez and Runkle, 2014). An unexpected cold front or "cold snap" may kill or stunt a cold-sensitive plant, due to low BTT, whereas cold-temperate and tolerant plants may develop normally (Ambroise, 2020). Acquired thermal tolerance encompasses plant adaptive responses to stressful or injurious temperatures, thus it is distinguished from BTT on a time-basis. Another distinction is the plastic nature of ATT versus the static nature of BTT. If a plant has low BTT for a given temperature range but exhibits high plasticity (i.e., effective ATT mechanisms), that plant may be able to acclimate to stressful temperatures given adequate time under stress (Suzuki et al., 2013).

Generally, low (≤ 10 °C) and high (≥ 35 °C) temperatures reduce primary productivity and induce stressed states in plants (Gote et al., 2009; Oquist, 1983). Plant stress or injury is classified as eustress or distress (Vázquez-Hernández, 2019). Eustress is essential in plant development, follows brief or gradual exposure to temperatures around T_b or T_m, and induces beneficial adaptation or developmental maturation (Ambroise, 2020). Distress follows prolonged or sudden exposure to T_b or lower, as well as to T_m or higher, and may diminish or arrest plant growth, development, and quality (Trudgill et al., 2005). Cold stress (CS) and cold injury (CI) are the stress states which occur during and following exposure to T_b or lower, while heat stress (HS) and heat injury (HI) occur around T_m or higher (Mahan et al., 1995). Thermal stress depends on the time-length and relative severity of a given temperature exposure, as well as plant species, cultivar, and developmental stage (Al-Huqail et al., 2020).

Acquired thermal tolerance encompasses all adaptive responses which follow exposure to stressful or injurious temperatures (Song, 2012). Stress or injury may induce ATT during long periods of gradual temperature change and short exposure to suboptimal temperature (Suzuki et al., 2013). Acquired thermal tolerance can improve plant growth, development, and metabolism at normal and stressful temperatures; as a result, single or repeat exposures may shift temperature response curves (Larkindale and Vierling, 2008). Cold-responsive (COR) and heat shock responsive (HSR) pathways represent the two general signaling and response pathways for BTT and ATT during CS and HS (Mueller, 2017). For instance, spinach grown in low air temperature (15/10 °C day/night) produced twice the concentration of Rubisco, fourfold the concentration of carbon, and greater leaf area compared with those grown in higher temperatures (30/25 °C

day/night) (Atkin and Tjoelker, 2003; Stinziano et al., 2019). On the other hand, thermal stress may impair a crop's subsequent productivity.

Thermal injury in nature typically follows rapid freezes, freeze-thaw cycles, intense summer heat, and prolonged or severe periods of CS or HS (Anyamba et al., 2002). Greenhouse-grown crops, on the other hand, primarily face thermal injury or stress due to failures or limitations of environmental control systems and extreme external conditions (Shamshiri et al., 2015). Thermal stress symptoms include wilted and discolored leaves, leaf senescence, stunted growth, delayed development, and necrotic tissue; as a result, crop quality and value diminish (Adhikari et al., 2022; Hassan et al., 2021). On the organismal scale, thermal stresses exacerbate other abiotic and biotic stresses, limit evapotranspiration, and impair long-distance signaling and nutrient transport (Kamatchi et al., 2024; Zhang et al., 2017). On the cellular to organellar scale, thermal stress disrupts the mechanical properties of membranes, the conformation and kinetics of enzymes and their reactions, and the availability and osmotic potential of water and mineral nutrients (Sage et al., 2015). Due to its widespread influence across all plant tissues, thermal stress shares common molecular biomarkers with other stressors and produces a strong cascade of signals (Hasanuzzaman et al., 2013). Molecular biomarkers provide mechanistic insights about CS and HS and include the following: cold and heat-shock proteins (CSPs, HSPs), proline, malondialdehyde (MDA), reactive oxygen species (ROS), dehydrins, and hormones (Ashraf, 2021). Because of our oxygen-rich atmosphere and oxygen's critical roles in biological systems, practically all sources of abiotic and biotic stress form ROS, albeit with stress-specific location and ROS types. Superoxide radical (O_2^-), hydrogen peroxide (H_2O_2), peroxide radical (OH^-), and singlet oxygen ($^1O_2$) are the primary ROS which form during stress cascades in plant cells (Foyer et al., 1997; Pospíšil and Prasad, 2014). Mitochondria, chloroplasts, and peroxisomes are the predominant sites of ROS generation, as over-reduction of photosynthetic or respiratory electron transport shuttles electrons to free oxygen in the reaction environment (Foyer and Hanke, 2022). Membrane-bound protein complexes called respiratory burst oxidase homologues (RBOHs) also generate ROS directly to initiate stress-signals (Chapman et al., 2019). As highly reactive and potent oxidizers, ROS directly damage membranes, proteins, DNA, as well as various secondary metabolites. Due to their widespread production throughout plants, high reactivity, and relative simplicity, ROS often serve as the first messenger to relay thermal stress (Suzuki and Mittler,

2006). During HS, ROS primarily accumulate in the cytosol and nucleus. Temperature stress reduces enzyme efficiency.

Hormonal biomarkers provide broad but efficient insight into plant stress responses, owing to their general ubiquity and the extensive literature detailing their roles. Hormones such as abscisic acid (ABA), jasmonic acid (JA), salicylic acid (SA), and ethylene (ET) are generally associated with stress responses; however, cytokinins (CK), auxins (AUX), gibberellins (GA), and brassinosteroids (BA) regulate general growth, developmental, and metabolic processes as well as stress responses (Castroverde and Dina, 2021). Temperature, drought, and light stress influence ABA, JA, and ET production in basil, and endogenous levels as well as exogenous application of JA and ABA in plant tissues underpins ATT at low temperatures (Frattiani et al., 2017; Hu et al., 2017; Larsen, 2023; Li et al., 2021).

Culinary Herb Production

Basil (*Ocimum* spp.) is the most popular culinary herb in the US, and sweet basil (*Ocimum basilicum)* is the widest-produced species (Simon et al., 1999). Green-leafed cultivars such as 'Nufar', 'Genovese', and 'Italian Large Leaf', as well as purple-leafed cultivars, such as 'Red Rubin' and 'Dark Opal', are commercially popular (Walters and Currey, 2015). The T_o for basil germination ranges from 25 to 30 ºC, depending on the cultivar. Some evidence suggests purple basil favors 20 to 25 ºC during germination, while green basil may germinate best in 25 to 30 ºC (Fallahi, 2015). Basil species are sensitive to low ambient temperatures, and they exhibit the highest leaf unfolding rate, yield the greatest shoot fresh and dry mass, and have the greatest leaf area in production air-temperatures of ≈29 ºC, compared with a T_b of ≈11 ºC (Al-Huqail et al., 2020; Barickman et al., 2021; Fallahi, 2015; Hendrickson et al., 2022; Walters and Currey, 2019). While basil is sensitive to low temperature, there is also an upper ceiling for ideal growth. Temperatures of 35 ºC and above generally reduce leaf number, shoot length, and fresh mass production when compared to temperatures ranging from 25 to 30 ºC (Al-Huqail et al., 2020). Basil's T_b of ≈11 ºC classifies it as a cold-sensitive species, and complicates winter-production of basil, as well as postharvest storage year-round. Nutrient solution heating may minimize air-heating costs and simultaneously improve basil growth during the cold season. Basil grown in 23 °C AT may benefit from a root zone temperature increase from 23 °C to 28 to 31 °C (Hendrickson et al., 2022). Barickman et al. (2021) found that basil subject to ≈32 °C ADT

produced shorter stems, less leaf dry mass, and lower leaf area compared to those grown in ≈26 °C, which agrees with the other authors' T_{opt} around 29 °C.

Cold stress and injury occur in basil when AT dips below 12 °C, and symptoms include wilted, browned, and dulled leaves; as a result, crop quality and salability diminish (Vitor et al., 2016). Compared with mild to optimal AT (≈15 to 30°C), basil grown in low temperature conditions (AT < 12°C) may synthesize more total phenolics, flavonoids, and essential oils to attenuate metabolic damage. In low AT (10 °C) basil roots and leaves produced more catalase, guaiacol-peroxidase, and pyrogallol-peroxidase, all of which scavenge free radicals, and could indicate an oxidative or stressed state (Hasanuzzaman et al., 2020).

During post-harvest storage, shipping companies and grocers must carefully balance tissue decay and microbial growth, which can occur at temperatures above 12 °C, with chilling stress and injury, which can occur in basil below 12 °C (Aharoni et. al., 2010). For instance, Lange and Cameron (1994) reported just 1- or 3-day shelf lives for fresh-cut basil stored in air temperatures of 0 or 5 °C, which are common in refrigerated produce trucks. Further, pre-harvest exposure to 10 °C AT for 4 h/d for 2 d doubled the shelf-life of basil stored in 0 and 5 °C. Other authors have reported similar shelf lives for basil stored in 4 and 12 °C (Fratianni et al., 2017).

Cilantro (*Coriandrum sativum*) is a culinary herb featured in many cuisines around the world. Cilantro grows best in warm temperatures. Fresh mass, dry mass, and height increased linearly with AT up to ≈ 24 °C, though heat-tolerant cultivars grew well in up to ≈29 °C (Mortensen, 2014; Currey et al., 2016). Nutrient solution temperatures around ≈25 °C were ideal for fresh mass production (Nguyen et al., 2019, 2020; Silva et al., 2020, 2022). Exposure to AT or RZT below or above 25 °C may stunt cilantro growth and development. Nguyen et al. (2019) found that cilantro grown with 15, 20, 30, or 35 °C NST produced less fresh weight, dry weight, and leaf area compared with those grown in 25 °C NST.

Parsley (*Petroselenium crispum*) is a Mediterranean herb, widely popular across the globe for culinary use. Previous authors demonstrated linear increases in parsley fresh mass and dry matter concentration when air temperature increased from 10 to 22 °C (Walters and Lopez, 2021; Frąszczak and Knaflewski, 2009). Air temperatures around 22 °C are difficult to maintain in greenhouses located in hot, humid regions, especially during the warm seasons. Eidsten and Giselrod (1985) observed 21°C AT T_o for biomass yield and height in parsley, with 24 °C NST T_o.

Sage (*Salvia* spp.) species are globally renowned for ornamental and culinary use. Nine hundred or more *Salvia* species exist in a variety of climates, which renders identification of a single set of cardinal temperatures for them all impossible (Wu et al., 2012). Most sage species are native to Mediterranean or arid climates and favor higher air temperatures, though some species may tolerate low temperatures. Moccaldi and Runkle (2007) reported a ≈7 °C T_b for biomass production in *Salvia splendens*, thus it is a cold-temperate crop. Common sage *(Salvia officinalis)* is the most popular culinary species in *Salvia* and favors ≈25 ± 2 °C ADT for optimal leaf mass yield (Ghorbani and Esmaeilizadeh, 2017; Mortensen, 2014; Walters and Lopez, 2023). On the other hand, *Salvia exserta* flowered later and grew more nodes and lateral shoots in 17 °C compared with 26 °C AT (Mata and Botto, 2011). Air temperatures > 29 °C induced HS in sage, but acclimation to hotter temperatures could attenuate yield reductions under HS. Natarajan et al. (2005) exposed two-week old *Salvia splendens* to 35 °C for 3 $h \cdot day^{-1} \cdot week^{-1}$ for three consecutive weeks (total 18 h exposure), then transferred them to greenhouses held at 30 and 35 °C AT, and found that plants preconditioned with 35 °C were shorter, had thicker stems, greater dry mass, and scored higher on market ratings, compared to those without preconditioning.

Culinary herb production in controlled environments is steadily growing in the US, however, air temperature control consumes much energy, and thus increases costs in cold or hot seasons. Nutrient solution temperature is often overlooked but can influence crop growth and could be regulated to improve energy use efficiency in suboptimal air temperatures. Thus, research which explores the relationship between nutrient solution temperature, air temperature, and culinary herb growth and development is beneficial for informing producers. Therefore, the objectives of this research were to determine the influence and interactions between air and nutrient solution temperatures on growth, development, shoot tissue mineral concentrations, and postharvest storage of basil, cilantro, parsley, and common sage. We hypothesized that as air and nutrient solution temperature approached the air temperature optimum. Chapter 2 focuses on the growth, development, and mineral nutrient responses and of basil, cilantro, parsley, and common sage to air and nutrient solution temperatures, while chapter 3 focuses on the post-harvest weight loss response of basil to air and nutrient solution temperatures.

Chapter II

Air and Nutrient Solution Temperature Influence the Growth, Development, and Mineral Nutrition of Five Culinary Herbs

Keywords: CEA, greenhouse, mineral nutrients

Abstract

Controlled environment agriculture (CEA) is a growing sector of specialty crop production, and greenhouses are a predominant type of CEA. Greenhouses may extend production seasons and enhance control over the growing environment, though control generally comes with elevated energy use. Culinary herbs are specialty crops which garner high value as fresh tissue. Air and root-zone temperatures affect herb growth, development, and tissue mineral concentrations but the interaction effects between those temperatures are unestablished for many herb species. If hydroponic producers could reduce air temperature control while maintaining comparable biomass yield and quality by modifying nutrient solution temperatures, they could spend less on energy. Therefore, the research objectives were to [1] quantify the effects of air and nutrient solution temperatures on growth, development, and shoot tissue mineral concentrations of four culinary herb species, and [2] determine the extent which air and nutrient solution temperatures interact to influence growth, development, and shoot mineral concentrations. To achieve our objectives, we grew basil (*Ocimum basilicum*) 'Nufar' and 'Red Rubin', cilantro (*Coriandrum sativum*) 'Santo', common sage (*Salvia officinalis*), and parsley (*Petroselenium crispum*) 'Giant of Italy' in 20 or 30 °C air temperature, utilizing deep-water-culture tanks with 15, 20, 25, 30, or 35 °C nutrient solution temperatures. Basil 'Nufar' and 'Red Rubin' grown in 30 °C air temperature with 30 °C nutrient solution temperature produced the greatest fresh and dry mass, the most nodes, and longest stems. Cilantro 'Santo' fresh mass, dry mass, and leaf number quadratically increased as nutrient solution temperature increased from 15 to 25 °C. Cilantro shoot length quadratically increased as nutrient solution temperature increased up to 25 °C, and it quadratically decreased then increased as air temperature increased from 20 to 30 °C. Common sage and parsley 'Giant of Italy' fresh mass, length, node number, and leaf number quadratically increased as nutrient solution temperature increased from 15 to 25 °C, then declined as nutrient solution temperature further increased to 35 °C. Thus, we recommend nutrient solution temperatures of 25 to 30 °C for basil production or 20 to 25 °C for cilantro, common sage, and parsley, for maximum biomass yield.

Introduction

Culinary herbs are high-value specialty crops with unique flavors and aromas. Herbs play a key role in cuisine, beauty products, and traditional medicines across the globe, largely owing

to the flavor and aroma compounds they produce (Nguyen, 2019; Spence, 2021). Large-scale field producers typically sell herbs for dry spice production, essential oil extraction, or fresh-cut use; on the other hand, smaller-scale controlled environment producers primarily grow high quality fresh-cut or potted herbs for culinary use. Fresh-cut herbs' flavors and aromas are superior to dried herbs, as the constituent flavor compounds are volatile, but fresh herbs degrade much quicker in storage (Prusinowska and Śmigielski, 2015).

The demand for fresh cut herbs at affordable prices and herbs' short shelf lives together invite a shift towards wider-spread production. Field production is space intensive, delimited by seasons, and cannot be implemented in highly urbanized areas; on the other hand, smaller-scale controlled environment production schemes can produce high quality herbs year-round and may minimize wasteful shipping.

Glass-glazed greenhouses are popular for food-crop production because glass is highly light-transmissive and has a long lifespan in the absence of extreme weather events. Glass is a poor insulator, though, which makes air temperature regulation energy-expensive; thus, the additional overhead reduces producers' profits. (Aguilar-Santana et al., 2020). In extreme conditions, producers may increase or decrease the maxima or minima for their temperature setpoints to reduce energy use, but plant growth is temperature sensitive. Evaporative cooling is a common strategy to reduce air temperatures; however, in hot and humid climates, evaporative strategies may fail to achieve the desired setpoints due to physical constraints such as low vapor pressure deficit. To scale controlled environment production sustainably while maintaining high crop quality and yields, we must develop strategies which minimize energy use without sacrificing crop growth and development (Guo et al., 2021).

The optimum temperature ranges for biomass production is 25 to 30 °C for basil (*Ocimum basilicum*), 24 to 26 °C for cilantro (*Coriandrum sativum*), 20 to 22 °C for parsley (*Petroselinum crispum*) and 24 to 27 °C for common sage (*Salvia officinalis*) (Al-Huqail et al. 2020; Hendrickson et al. 2022; Mortensen 2014; Walters and Currey, 2019; Walters and Lopez, 2021). Above or below the optimum temperature (T_o), plant biomass production is reduced; thus, producers must strive to achieve those temperatures if the primary goal desired is high biomass yield (Aharoni et al., 2010).

In hydroponic systems, plants' root-zones are submerged in a nutrient solution comprised primarily of water, which is supplemented with mineral nutrients and a dissolved oxygen source.

Water has high thermal inertia and changes temperature more slowly than air. Heated or cooled nutrient solutions leverage that principle and could be implemented in tandem with reduced air temperatures to minimize overall energy use without sacrifice to plant yield and quality (De Lima et al., 2021). Despite many studies which describe the influence of air temperature on culinary herb growth and development (Barickman et al., 2021; Hendrickson et al., 2022; Nguyen et al., 2019, 2020; Silva et al., 2020, 2022), there is sparse research which details the influence of nutrient solution temperature on culinary herb growth and development, and less still which explore the interaction between air and nutrient solution temperatures on culinary herb growth and development. Therefore, our objective was to determine the extent air and nutrient solution temperatures affect the growth, development, and shoot mineral concentrations of basil, cilantro, sage, and parsley.

Materials and Methods

Plant Production

Thirteen seeds (Johnny's Seeds, Winslow, ME) of basil 'Nufar' and 'Red Rubin', cilantro 'Santo', parsley 'Giant of Italy', and common sage were sown per cell of dry phenolic foam substrate (162 count Oasis® Horticubes® 1" multi-seed; Smithers Oasis, Kent, OH). After sowing, flats were placed into ebb-and-flow hydroponic systems in two greenhouse bays with target ATs of 20 and 30 °C. Average daily air temperatures (ADT °C) measured during production of each species and cultivar are listed in Table 1.

Seedlings were fertigated daily with nutrient solution comprised of reverse-osmosis (RO) water with 12N-1.8P-13.4K water-soluble fertilizer titrated to concentrations as follows ($mg \cdot L^{-1}$): 100 nitrogen, 15 phosphorus, 112 potassium, 58 calcium, 17 magnesium, 2 sulfur, 1.4 iron, 0.5 zinc, 0.4 copper, 0.4 manganese, 0.1 boron, and 0.1 molybdenum (RO Hydro FeED; JR Peters, Inc., Allentown, PA), and magnesium sulfate ($MgSO_4 \cdot 7H_2O$) (TwinsBridge International, Englewood, NJ) providing ($mg \cdot L^{-1}$) 15 magnesium and 20 sulfur. Electrical conductivity (EC) and pH were monitored (HI9813-6N Portable Waterproof pH/EC/TDS Meter; Hanna Instruments, Woonsocket, RI) and pH was adjusted to 5.8 using sulfuric acid (H_2SO_4) or potassium bicarbonate ($KHCO_3$).

Ten (basil 'Nufar'), 17 (basil 'Red Rubin' and cilantro 'Santo'), and 22 (parsley 'Giant of Italy' and common sage) days after sowing (DAS), we thinned seedlings to 8 ± 1 plants per cell based on Li et al. (2024). Thirty-five representative cells of each species per treatment were

transplanted into a 61 × 122 cm Styrofoam raft (Lettuce rafts; Beaver Plastics, Ltd., St. Acheson, Alberta, Canada), which floated atop 122 × 183 × 18 cm deep-water-culture (DWC) hydroponic systems. Ten representative cells per species or cultivar per treatment were harvested for destructive measurements at the end of the growing cycle; whereas the remaining cells were used for postharvest storage, tolerance for error, and to ensure consistent plant spacing.

Nutrient solutions consisted of RO water, 12N-1.8P-13.4K fertilizer, and $MgSO_4$ all titrated to twice the reported concentrations for propagation. Air pumps (AAPA45L; Hydrofarm, New Hudson, MI) and air stones (AA-STONE-ROUND; Hydrofarm, New Hudson, MI) provided dissolved oxygen in each solution. Our NST targets were 15, 20, 25, 30, and 35 °C.

Environmental Conditions

This experiment was set up as a factorial design, with two air temperature setpoints and five nutrient solution temperature setpoints. Two identical greenhouse compartments were used, one for each air temperature. Within each compartment, there were five DWC hydroponics systems per cultivar, one per NST.

Targets for average daily air temperature were 20 and 30 °C with a +5 °C DIF. Thus, with a 16-h photoperiod, target day temperatures (°C) were 23 ± 2 °C and 33 ± 2 °C and night temperatures were 18 ± 2 °C and 28 ± 2 °C. Air temperatures (AT) were measured with a thermistor housed within an aspirated radiation shield (EE08 temperature sensor, ST-110 thermistor; Apogee Instruments, Logan, UT), logged by a datalogger (CR1000x; Campbell Scientific, Logan, UT), and mean values are reported in Table 1. Exhaust fans, evaporative-pad cooling, shade curtains, central steam heating, horizontal air flow fans, and supplemental lighting (450-watt high pressure sodium) regulated the greenhouse environment under the control of an environmental control system (Priva Maximizer™; Priva North America, Vineland Station, ON, Canada).

Five NST targets of 15, 20, 25, 30, and 35 °C were maintained by chillers (1/10 hp or 1/4 hp chillers; Active Aqua, Petaluma, CA) or heaters (ISTA I-H616; Tzong Yang Aquarium Co., Tainan City, Taiwan) connected in-line with a circulating pump (AAPW250 or AAPW400; Hydrofarm, New Hudson, MI). Actual NSTs were measured with a submerged thermistor (ST100; Apogee Instruments, Logan, UT) and leaf temperatures were measured with infrared radiometers (SI-131 SSL; Apogee Instruments). Infrared radiometers measured leaf temperatures of basil ‘Nufar’ and common sage only, due to equipment restraints. Each minute, a datalogger

(CR1000x; Campbell Scientific) logged the output of each sensor. Measured temperature values are reported in **Table 1**.

The production photoperiod was 16 h (0600 to 2200 HR), consisting of natural sunlight (lat. 35 °N) supplemented with day-extension high pressure sodium lamps to achieve target daily light integrals 1 (DLIs) of 14 ± 1 ($mol \cdot m^{-2} \cdot d^{-1}$), and quantum sensors (SQ-500; Apogee Instruments) measured light intensities in each bay. Table 1 contains the measured DLIs.

Data Collection

Plants were harvested 15 (basil 'Nufar'), 18 (basil 'Red Rubin'), and 22 (cilantro 'Santo', parsley 'Giant of Italy' and common sage) days after transplant. The number of days of treatment for each crop corresponded to the time to reach marketable size. We collected measurements on 10 cells (6 to 8 plants per cell) per species grown in each treatment combination (AT × NST) for each replication. We measured plant height from the substrate to the top of the tallest leaf (PL) (cilantro, parsley), individual plant height (PH) from the substrate to the apical meristem (basil, common sage), total cell fresh mass, individual plant fresh mass (FM) (basil, common sage), leaf number (LN) (cilantro, parsley), and node number (NN) (basil, common sage). Entire cilantro and parsley shoots and basil leaves and stems were oven-dried (60 °C, ≥3 days) and weighed. We recorded dry weights of whole plants, regarded as shoot dry mass (SDM) (cilantro), along with separate leaf and stem dry masses (LDM, STDM) (basil 'Nufar' and 'Red Rubin'). Basil stem and leaf dry masses for each sample were added together to produce basil SDM values. Dry matter concentration (DMC) for basil and cilantro were calculated by dividing each sample's SDM by its FM and multiplying by 100 to generate a percent weight value (%DM/FM). The equation is as follows:

$$DMC\ (\%w/w) = (SDM \cdot FM^{-1}) \cdot 100$$

Leaf to stem ratio (LSR) was calculated by dividing each basil sample's LDM by its STDM.

$$LSR\ (w/w) = LDM \cdot STDM^{-1}$$

Internode length (IL) was calculated by dividing each basil and common sage sample's NN by its PH.

$$IL\ (cm) = NN \cdot PH^{-1}$$

Dry shoot samples of basil 'Nufar' and 'Red Rubin' and cilantro 'Santo' were pulverized with mortar and pestle, then reweighed as 0.3 g samples, placed in air-tight plastic centrifuge tubes,

Table 1. Average daily air temperature, nutrient solution temperature, relative humidity, and daily light integral (± standard error of the mean) are displayed for basil (Ocimum basilicum) 'Nufar' and 'Red Rubin', cilantro (Coriandrum sativum) 'Santo', parsley (Petroselenium crispum) 'Giant of Italy', and common sage (Salvia officinalis). [X]RH= Relative Humidity, [Y]DLI = daily light integral, [Z]Dash lines = no data, *missing data

Rep.	Temperature (°C)			RH[X] (%)	DLI[Y] ($mol \cdot m^{-2} \cdot d^{-1}$)	Temperature (°C)			RH (%)	DLI ($mol \cdot m^{-2} \cdot d^{-1}$)
	Air	Solution	Leaf			Air	Solution	Leaf		
	Basil 'Nufar' (*Ocimum basilicum*)					Basil 'Red Rubin' (*Ocimum basilicum*)				
1	22.3 ±0.4	16.4 ±2.2	22.4 ±0.5	69.6 ±3.2	12.1 ±0.9	22.3 ±0.5	16.4 ±2.0	--	69.8 ±3.5	12.0 ±0.8
	--[Z]	20.7 ±1.0	23.6 ±0.4	--	--	--	20.8 ±1.0	--	--	--
	--	24.3 ±0.9	23.9 ±1.0	--	--	--	24.5 ±0.9	--	--	--
	--	28.6 ±2.4	24.2 ±0.5	--	--	--	28.7 ±2.3	--	--	--
	--	32.3 ±3.8	24.7 ±1.1	--	--	--	32.7 ±3.6	--	--	--
	27.0 ±1.3	16.3 ±3.6	26.0 ±1.0	52.1 ±1.4	15.0 ±1.0	27.2 ±1.3	16.3 ±3.8	--	52.2 ±1.7	14.8 ±1.0
	--	21.4 ±2.0	26.5 ±1.2	--	--	--	21.3 ±1.8	--	--	--
	--	26.2 ±0.5	26.9 ±0.7	--	--	--	26.2 ±0.4	--	--	--
	--	29.3 ±1.3	-	--	--	--	29.4 ±1.2	--	--	--
	--	31.6 ±2.2	28.0 ±1.9	--	--		31.8 ±2.1	--	--	--
2	20.3 ±1.2	14.6 ±0.5	20.5 ±1.5	56.0 ±7.2	12.3 ±1.1	20.0 ±1.3	14.5 ±0.5	--	50.3 ±11.6	12.3 ±0.9
	--	19.9 ±0.1	21.1 ±1.1	--	--	--	19.8 ±0.2	--	--	--
	--	23.9 ±0.2	21.3 ±1.0	--	--	--	24.0 ±0.3	--	--	--
	--	29.8 ±0.1	21.6 ±1.1	--	--	--	29.8 ±0.1	--	--	--
	--	35.0 ±0.2	22.5 ±2.7	--	--		35.0 ±0.1	--	--	--
	28.5 ±1.5	15.6 ±1.1	26.2 ±1.0	37.8 ±6.3	15.6 ±3.8	28.6 ±1.0	15.4 ±1.0	--	34.7 ±5.5	16.0 ±3.2
	--	20.1 ±0.4	26.6 ±1.0	--	--	--	20.1 ±0.3	--	--	--
	--	24.4 ±0.7	26.9 ±1.0	--	--	--	24.4 ±0.6	--	--	--
	--	30.1 ±0.2	26.9 ±1.5	--	--	--	30.2 ±0.2	--	--	--
	--	34.6 ±0.4	27.5 ±1.6*	--	--	--	34.7 ±0.8	--	--	--
3	19.3 ±0.7	14.8 ±1.8	19.3 ±1.3	45.2 ±9.0	14.7 ±1.2	19.2 ±0.7	14.7 ±1.7	--	44.8 ±8.8	14.7 ±1.1
	--	21.7 ±0.2	20.9 ±0.9	--	--	--	21.7 ±0.2	--	--	--
	--	25.1 ±0.5	21.1 ±1.6	--	--	--	25.1 ±0.5	--	--	--
	--	29.4 ±0.2	21.2 ±1.1	--	--	--	29.4 ±0.3	--	--	--
	--	33.9 ±0.2	21.2 ±0.8	--	--	--	33.9 ±0.3	--	--	--
	29.7 ±0.6	14.4 ±3.6	27.8 ±3.2	30.5 ±7.9	10.8 ±0.8	29.5 ±0.6	14.4 ±3.2	--	30.6 ±7.9	10.8 ±0.8*
	--	21.6 ±2.0	28.1 ±3.0	--	--	--	21.5 ±1.9	--	--	--
	--	26.6 ±1.3	28.4 ±3.2	--	--	--	26.5 ±1.2	--	--	--
	--	31.6 ±1.0	29.1 ±3.6	--	--	--	31.6 ±0.9	--	--	--
	--	32.9 ±1.1	29.2 ±3.2	--	--	--	33.4 ±1.4	--	--	--
	Cilantro 'Santo' (*Coriandrum sativum*)					Common Sage (*Salvia officinalis*) and Parsley 'Giant of Italy' (*Petroselenium crispum*)				
1	21.8 ±1.2	15.8 ±2.3	--	66.5 ±8.2	12.0 ±0.8	19.8 ±0.9	14.3 ±0.3	--	--[y]	13.1 ±3.1
	--	20.8 ±0.9	--	--	--	--	23.3 ±0.9	--	--	--
	--	24.7 ±0.9	--	--	--	--	24.6 ±0.5	--	--	--
	--	28.9 ±2.1	--	--	--	--	30.5 ±0.4	--	--	--
	--	33.1 ±3.3	--	--	--	--	35.3 ±0.2	--	--	--

Table 1. Continued

	26.9 ±1.4	16.1 ±3.5	--	50.7 ±4.0	14.8 ±1.1	--	--	--	--	--
	--	21.2 ±1.7	--	--	--	--	--	--	--	--
	--	26.2 ±0.4	--	--	--	--	--	--	--	--
	--	29.5 ±1.1	--	--	--	--	--	--	--	--
	--	32.0 ±1.9	--	--	--	--	--	--	--	--
2	20.0 ±1.3	14.7 ±0.8	--	50.9 ±10.6	12.1 ±1.2	19.8 ±2.4	15.2 ±1.2	--	--	13.7 ±2.2
	--	19.8 ±0.4	--	--	--	--	19.0 ±0.6	--	--	--
	--	24.1 ±0.4	--	--	--	--	28.3 ±1.1	--	--	--
	--	29.7 ±0.3	--	--	--	--	29.1 ±0.1	--	--	--
	--	34.8 ±0.7	--	--	--	--	35.2 ±0.1	--	--	--
	28.3 ±1.4	15.6 ±1.4	--	35.9 ±6.2	16.2 ±3.2	--	--	--	--	--
	--	20.3 ±0.9	--	--	--	--	--	--	--	--
	--	24.5 ±0.9	--	--	--	--	--	--	--	--
	--	30.3 ±0.3	--	--	--	--	--	--	--	--
	--	34.9±1.0	--	--	--			--	--	--
3	19.1 ±0.7	14.7 ±1.6	--	46.8 ±10.1	14.6 ±1.1	21.8 ±1.7	16.4 ±0.8	--	--	11.6 ±2.5
	--	21.6 ±0.2	--	--	--	--	17.1 ±1.8	--	--	--
	--	25.0 ±0.7	--	--	--	--	29.1 ±0.5	--	--	--
	--	29.5 ±0.3	--	--	--	--	30.9 ±0.8	--	--	--
	--	33.5 ±1.4	--	--	--	--	33.9 ±0.4	--	--	--
	29.1 ±1.5	14.5 ±2.9	--	32.8 ±8.9	10.8 ±0.8*	--	--	--	--	--
	--	21.4 ±1.7	--	--	--	--	--	--	--	--
	--	26.4 ±1.1	--	--	--	--	--	--	--	--
	--	31.4 ±1.0	--	--	--	--	--	--	--	--
	--	33.6 ±1.5	--	--	--			--	--	--

and sent to the U.S. Department of Agriculture, Agricultural Research Service (USDA-ARS) in Toledo, OH for mineral analyses.

Mineral Analyses

Mineral analyses were conducted in accordance with the protocol outlined by Boldt and Altland (2021) to quantify dry shoot tissue concentrations (% w/w or $mg \cdot g^{-1}$) of carbon (C), nitrogen (N), potassium (K), phosphorus (P), calcium (Ca), magnesium (Mg), sulfur (S), as well as ($\mu g \cdot g^{-1}$) boron (B), copper (Cu), iron (Fe), manganese (Mn), molybdenum (Mo), and zinc (Zn) in basil 'Nufar' and 'Red Rubin' and cilantro 'Santo'. For N analysis, subsamples (2.5 mg) of the dried, homogenized tissue of each species were weighed into tin containers (EA Consumables, Marlton, NJ) and placed into a CHN analyzer (vario MICRO cube; Elementar, Hanau, Germany). All other minerals (K, P, Ca, Mg, S, B, Cu, Fe, Mn, Mo, and Zn) required tissue digestion (modified Environmental Protection Agency method 3051) prior to assay. Subsamples (0.25 g) of dry and homogenized tissue from each species were suspended in 5 mL of nitric acid in Teflon vessels. The acid-tissue mixture was gradually microwave-heated (MARS 6; CEM Corp., Matthews, NC) up to 200 °C over 20 minutes (min) and held at 200 °C (20 additional min). The vessels were then cooled to room temperature and supplemented with 1.5 mL of hydrogen peroxide (H_2O_2), then again heated to 200 °C (for 20 min), and allowed to return to room temperature. Samples were washed with 12 mL of ultrapure (18 MΩ·cm) water, then filtered through cellulose paper (Whatman #2). Subsamples (1.3 mL) of the supernatant were diluted with 8.7 mL of 18 MΩ·cm water), then analyzed with inductively coupled plasma optical emission spectroscopy (ICP-OES; iCAP 6300 Duo, Thermo Electron Corp., Waltham, MA). Each digestion carousel containing the experimental samples included external standards (Spinach leaf, NIST standard reference material 1570a; and Peach leaf, NIST standard reference material 1547) which were assayed periodically on intervals of 1:20 (1570a: experimental sample) and 1:40 (1547: experimental sample).

Experimental Design and Statistical Analyses

Treatments consisted of a factorial combination between two air temperatures (AT) (20 or 30 °C) and five nutrient solution temperatures (NST) (15, 20, 25, 30, or 35 °C), repeated three times over time, for basil 'Nufar' and 'Red Rubin', and cilantro 'Santo'. Common sage and parsley 'Giant of Italy' only had one AT (20 °C), with 15, 20, 25, 30, or 35 °C NST. During each harvest, morphological data were collected on 80 plants per treatment combination (10 cells,

each containing 8 plants per cell) for each replication. In total, 240 plants were sampled per treatment combination per species. Due to differences in actual ATs and NSTs from the target setpoints between replications, actual measured air (6) and nutrient solution (15) temperatures were used for statistical analyses.

We conducted preliminary analysis of variance (ANOVA) tests for each response variable using JMP v15 (SAS Institute Inc., Cary, NC) with the least squares means method, with a full factorial combination of main effects. This guided us on how to subsequently proceed with regression analysis. When ANOVA interaction effects were insignificant ($P \geq 0.05$), we pooled the data for regression analysis. Surface regression analysis was evaluated when the interaction was significant, and linear and quadratic regression were evaluated when the main effects were significant. Regression analyses were analyzed using SigmaPlot (version 15, Systat Software Inc., San Jose, CA), and the equations used to generate the surface regression models were adapted from Walters and Lopez (2021). The full equation for the statistical model interaction effects between air and nutrient solution temperature on each growth parameter was as follows:

Surface regression: $f(x) = y0 + a \cdot x + b \cdot y + c \cdot x^2 + d \cdot y^2 + e \cdot x \cdot y$

x = AT °C, y = NST °C

For parameters with only significant main effects, linear and quadratic relationships were evaluated using the following equations:

Linear: $y = y0 + a \cdot x$

Quadratic: $y = y0 + a \cdot x + b \cdot x^2$

Linear, quadratic, and surface regression results for growth parameters are reported in **Table 2**, while those corresponding to tissue mineral concentrations are in **Table 3**.

Results

All percentage and unit values which describe any given response in this document henceforth were calculated via substitution of target values for AT (x) and NST (y) and the regression results for each model term otherwise ($y0$, a, b, c, d, e) into either the surface (e, $P < 0.05$), quadratic (e, $P > 0.05$; b, $P < 0.05$), or linear regression (e, $P > 0.05$; b, $P > 0.05$) equation provided on page 19. Thus, all values referenced herein are subject to model error and are not

Table 2. Linear, quadratic, and surface regression coefficients for basil (Ocimum basilicum) 'Nufar' and 'Red Rubin', cilantro (Coriandrum sativum) 'Santo', parsley (Petroselenium crispum) 'Giant of Italy', and common sage (Salvia officinalis) growth and development responses to air and nutrient solution temperatures. Letters as superscripts designate the following: [Z]Coefficients for model equations; [Y]Dash lines = 0; [X]Standard error of the mean; [W]Fresh mass; [V]Shoot dry mass; [U]Leaf dry mass; [T]Stem dry mass; SPH = Plant height or SL = Shoot length; [R]Internode length; [Q]Leaf to stem ratio; [P]Node number; ODry matter concentration. Statistical model: $\{f(x) = y0 + a \cdot x + b \cdot y + c \cdot x^2 + d \cdot y^2 + e\}$

	Basil 'Nufar' (*Ocimum basilicum*)									
	FM[W] (g)	SDM[V] (g)	LDM[U] (g)	STDM[T] (g)	PH[S] (cm)	IL[R] (cm)	LSR[Q] (%w/w)	NN[P] (#)	DMC[O] (%w/w)	
									AT	NST
y0	-312.0[Z]	-19.9	-13.1	-6.85	-125.0	-20.8	80.0	-24.90	9.49	23.2
a	22.4	1.51	0.998	0.514	9.36	1.62	-5.00	1.97	-0.105	--
b	2.89	0.124	0.0812	0.0428	0.937	0.184	-0.818	0.199	--[Y]	-1.22
c	-0.468	-0.0307	-0.0203	-0.0104	-0.186	-0.032	0.0899	-0.0381	--	--
d	-0.095	-0.0043	-0.0029	-0.0014	-0.0270	-0.0052	0.0121	-0.0046	--	0.0214
e	0.096	0.0044	0.0030	0.0012	0.0213	0.0041	0.0065	0.00180	--	--
R^2	0.78	0.70	0.68	0.71	0.67	0.51	0.74	0.51	0.08	0.67
SEM[X]	3.47	0.35	0.16	0.11	1.80	0.700	1.13	0.600	1.50	0.900

	Basil 'Red Rubin' *(Ocimum basilicum*)										
	FM (g)	SDM (g)	LDM (g)	STDM (g)	PH (cm)	IL (cm)	LSR (%w/w)	NN (#)		DMC (%w/w)	
								AT	NST	AT	NST
y0	-276.0	-19.1	-12.1	-7.002	-191.0	-12.3	46.7	1.29	-53.1	0.268	0.132
a	20.3	1.43	0.922	0.516	15.3	1.06	-3.42	0.265	--	-0.002	--
b	1.78	0.115	0.0669	0.0497	0.787	0.086	0.0651	--	4.64	--	-0.004
c	-0.41	-0.0284	-0.0183	-0.0102	-0.302	-0.0207	--	-0.005	--	$3.00 \cdot 10^{-4}$	--
d	-0.063	-0.0038	-0.0024	-0.0015	-0.0226	-0.0027	--	--	-0.091	--	$7.13 \cdot 10^{-5}$
e	0.077	0.004	0.0028	0.0013	0.0181	0.0026	--	--	--	--	--
R^2	0.79	0.79	0.79	0.75	0.65	0.48	0.82	0.02	0.49	0.08	0.17
SEM[X]	5.94	0.37	0.25	0.14	4.0	0.60	0.55	1.7	1.2	0.01	0.01

	Cilantro 'Santo' *(Coriandrum sativum*)				
	FM[W] (g)	SDM[V] (g)	SL[S] (cm)	LN[P] (#)		DMC (%w/w)
				AT	NST	
y0	-119.0	-4.75	23.2	-1.76	2.15	13.8
a	15.7	0.77	-4.67	0.681	--	1.17
b	--	--	5.91	--	0.401	-1.88
c	-0.339	-0.0163	0.119	-0.01	--	-0.0293
d	--	--	-0.113	--	-0.01	0.038
e	--	--	-0.0359	--	--	0.0096
R^2	0.58	0.29	0.62	0.04	0.04	0.58
SEM[X]	12.09	0.99	4.3	1.7	1.7	1.73

	Common Sage *(Salvia officinalis)*			
	FM[W] (g)	PH[S] (cm)	IL[R] (cm)	NN[P] (#)
y0	-51.4	5.62	1.40	4.04
a	--	--	--	--
b	6.84	0.799	0.101	0.137

Table 2. Continued

c	--	--	--	--
d	-0.137	-0.018	-0.002	-0.003
R^2	0.40	0.03	0.02	0.02
SEM^X	6.91	5.3	0.6	1.10
	Parsley 'Giant of Italy' (*Petroselenium crispum)*			
	FM^W (g)	PH^S (cm)		LN^P (#)
y0	-87.5	-22.6		1.22
a	--	--		--
b	11.0	4.99		0.214
c	--	--		--
d	-0.234	-0.103		-0.004
R^2	0.49	0.51		0.05
SEM^X	10.2	4.6		0.70

Table 3. Linear, quadratic, and surface regression coefficients for basil 'Nufar' and 'Red Rubin', cilantro 'Santo' dry shoot concentrations responses to air and nutrient solution temperatures. Letters as superscripts designate the following: [Z]Coefficients for model equations used to generate Figs. 1, 4, 7, 11, and 12; [Y]Dash lines = 0; [X]Carbon; [W]Nitrogen; [V]Phosphorus; [U]Potassium; [T]Calcium; [S]Magnesium; [R]Sulfur; [Q]Boron; [P]Copper; [O]Iron; [N]Manganese; [M]Molybdenum; and [L]Zinc. Statistical model: $\{f(x) = y0 + a \cdot x + b \cdot y + c \cdot x^2 + d \cdot y^2 + e \cdot x \cdot y\}$ [x = AT °C] [y = NST °C].

	Basil 'Nufar'									
	C^X (% w/w)		N^W (% w/w)		P^V (% w/w)	K^U (% w/w)		Ca^T (% w/w)	Mg^S (% w/w)	S^R (% w/w)
	AT	NST	AT	NST		AT	NST			
y0	15.864	41.95	16.858	2.047	3.123	39.576	1.372	-6.704	1.944	2.414
a	2.155	--	-1.047	--	-0.276	-2.887	--	0.501	-0.132	-0.183
b	--	-0.16	--	0.239	0.072	--	0.422	0.180	0.020	0.018
c	-0.050	--	0.023	--	0.007	0.062	--	-0.008	0.003	0.004
d	--	--	--	-0.004	-7.00E-05	--	-0.008	-0.001	-7.40E-05	-0.0001
e	--	--	--	--	-0.0021	--	--	-0.005	-0.001	-0.001
R^2	0.31	0.23	0.29	0.24	0.34	0.41	0.13	0.28	0.25	0.52

	B^Q (µg·g^{-1})	Cu^P (µg·g^{-1})	Fe^O (µg·g^{-1})	Mn^N (µg·g^{-1})	Mo^M (µg·g^{-1})	Zn^L (µg·g^{-1})
			NST			NST
y0	71.869	34.871	77.747	-159.562	-4.281	-41.897
a	-4.555	-4.795	--	5.270	0.350	--
b	0.197	2.283	0.860	13.894	0.016	8.907
c	0.119	0.122	--	0.114	-0.005	--
d	0.021	-0.020	--	-0.025	0.002	-0.154
e	-0.039	-0.035	--	-0.387	-0.004	--
R^2	0.50	0.46	0.10	0.36	0.59	0.202

	Basil 'Red Rubin'									
		N^W (% w/w)	P^V (% w/w)	K^U (% w/w)		Ca^T (% w/w)	Mg^S (% w/w)	S^R (% w/w)		
		NST	AT	AT	NST			AT	NST	
y0		2.299	10.579	30.348	6.495	-0.620	3.423	2.066	0.518	
a		--	-0.795	-2.057	0.032	0.122	-0.240	-0.143	--	
b		0.217	--	--	--	0.071	0.001	--	-0.017	
c		--	0.016	0.044	--	-0.002	0.005	0.003	--	
d		-0.004	--	--	--	-0.001	0.0002	--	0.0003	
e		--	--	--	--	-0.002	-0.001	--	--	
R^2		0.53	0.60	0.51	0.08	0.28	0.48	0.43	0.11	

	B^Q (µg · g^{-1})	Cu^P (µg · g^{-1})		Fe^O (µg · g^{-1})	Mn^N (µg · g^{-1})		Mo^M (µg · g^{-1})	Zn^L (µg · g^{-1})	
		AT	NST		AT	NST		AT	NST
y0	135.495	92.175	-16.159	859.099	556.82	79.770	2.488	-462.080	-100.887
a	-8.397	-7.006	--	-63.195	-35.868	--	-0.212	48.432	--
b	-0.705	--	1.671	12.312	--	1.417	0.027	--	13.470
c	0.120	0.144	--	1.266	0.708	--	0.005	-1.028	--
d	0.044	--	-0.024	-0.008	--	--	0.001	--	-0.218
e	-0.055	--	--	-0.399	--	--	-0.001	--	--
R^2	0.54	0.086	0.68	0.77	0.48	0.29	0.70	0.16	0.58

Table 3. Continued

	Cilantro 'Santo'										
	C^X (% w/w)		N^W (% w/w)		P^V (% w/w)		K^U (% w/w)	Ca^T (% w/w)	Mg^S (% w/w)	S^R (% w/w)	
	AT	NST	AT	NST	AT	NST		NST	NST	AT	NST
y0	42.458	44.268	25.616	3.419	4.717	0.398	38.138	0.094	0.476	0.404	0.246
a	-0.120	--	-1.703	--	-0.331	--	-3.282	--	--	-0.005	--
b	--	-0.641	--	0.308	--	0.049	0.814	0.075	-0.0026	--	0.009
c	--	--	0.035	--	0.007	--	0.073	--	--	--	--
d	--	0.017	--	-0.008	--	-0.001	-0.015	-0.002	--	--	-0.0003
e	--	--	--	--	--	--	-0.009	--	--	--	--
R^2	0.05	0.44	0.08	0.51	0.11	0.44	0.51	0.25	0.10	0.15	0.42

	B^Q ($\mu g \cdot g^{-1}$)		Cu^P ($\mu g \cdot g^{-1}$)	Fe^O ($\mu g \cdot g^{-1}$)		Mn^N ($\mu g \cdot g^{-1}$)		Mo^M ($\mu g \cdot g^{-1}$)	Zn^L ($\mu g \cdot g^{-1}$)	
	AT	NST		AT	NST	AT	NST	NST	AT	NST
y0	-98.099	-0.050	41.830	103.294	125.893	1214.677	-263.566	-5.478	825.079	-224.231
a	11.89	--	-4.836	-1.225	--	-94.256	--	--	-62.599	--
b	--	2.948	2.068	--	-2.105	--	31.924	0.601	--	28.628
c	-0.241	--	0.090	--	--	1.921	--	--	1.270	--
d	--	-0.043	-0.05	--	--	--	-0.664	-0.011	--	-0.623
e	--	--	0.014	--	--	--	--	--	--	--
R^2	0.06	0.49	0.58	0.06	0.50	0.14	0.36	0.52	0.08	0.45

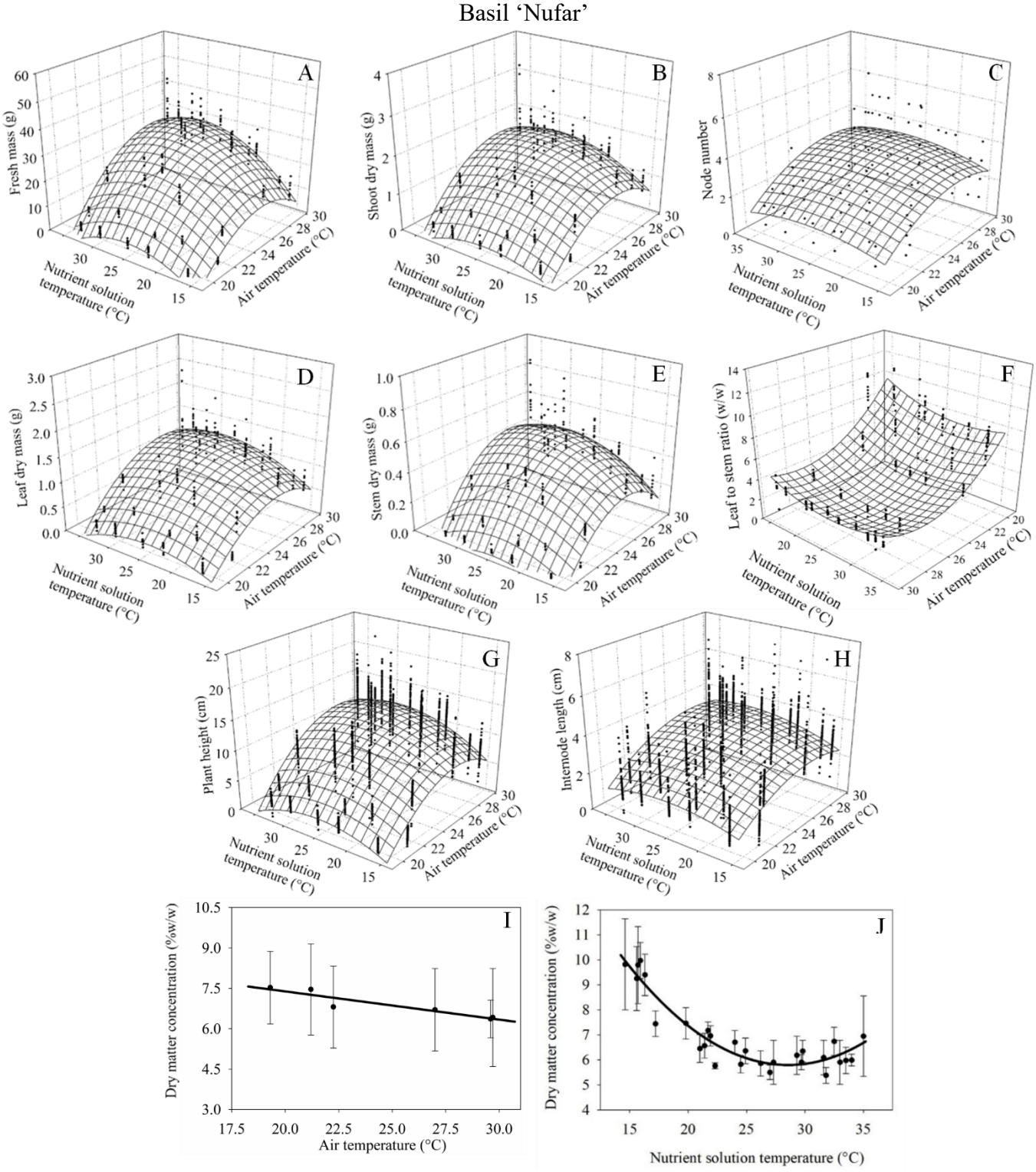


Figure 1. Basil (*Ocimum basilicum*) 'Nufar' air temperature and nutrient solution temperature interaction effects on fresh mass (A), shoot dry mass (B), node number (C), leaf dry mass (D), stem dry mass (E), leaf to stem ratio (F; axes are transposed), plant height (G), and internode length (H), and main effects dry matter concentration (I, J).

directly measured values. For all growth and development responses, as well as shoot micronutrient (Cu, B, Fe, Mn, Mo, and Zn) concentrations, the percent values represent the magnitude of the difference between the treatment combinations which were compared for a given response. Macronutrient (N, P, K, Ca, and S) shoot concentrations were reported as percent values which represent the direct difference, and not the relative magnitude of that change, between the treatment combinations compared for the given response.

Basil 'Nufar'

Air and nutrient solution temperature interacted to influence basil 'Nufar' fresh mass (FM), shoot dry mass (SDM), leaf dry mass (LDM), stem dry mass (STDM), leaf to stem dry mass ratio (LSR), shoot height (SH), node number (NN), and internode length (IL) (**Table 2, Fig. 1A-H**). In general, as AT increased to 30 °C and NST increased to 25 to 30 °C, FM, SDM, LDM, STDM, SH, and NN quadratically increased, then decreased; while LSR quadratically decreased, then increased.

Overall, basil 'Nufar' grown in 30 °C AT and 30 °C NST was calculated to produce the greatest FM, SDM, LDM, STDM, SH, and IL. In 20 °C AT, FM, SDM, LDM, STDM, SH, and IL increased as NST increased from 15 to 25 °C. Conversely, plants grown in 30 °C AT with 25 °C NST produced the lowest LSR, and those grown in 20 °C AT had a decrease in LSR as NST increased from 15 to 35 °C. Green basil grown in 20 °C AT and 25 °C NST were calculated to produce 164% (0.40 g) greater SDM, 104% (0.30 g) more LDM, 491% (0.16 g) more STDM, 48% (2.8 cm) greater SH, 31% (0.5) larger NN, 37% (0.6 cm) greater IL, and 24% lower LSR compared with those grown in 15 °C NST. On the other hand, those grown in 30 °C AT with 30 °C NST were calculated to produce 467% (22.5 g) greater FM, 142% (0.94 g) greater SDM, 118% (0.61 g) more LDM, 390% (0.24 g) more STDM, 96% (5.4 cm) greater SH, 27% larger NN, 47% (1.1 cm) greater IL, and 27% lower LSR compared with those grown in 15 °C NST. Plants grown in 20 °C AT with 25 °C NST produced 36% greater FM than those grown in 20 °C AT with 20 °C NST.

Dry matter concentration (DMC) decreased linearly as AT increased and decreased quadratically as NST increased to 25 to 30 °C, then increased as NST increased to 35 °C (**Fig. 1I-J**). Plants grown in 30 °C AT were calculated to have 14% lower DMC than those grown in 20 °C AT. In 25 °C NST, DMC was 51% lower compared to 15 °C NST.

Air and nutrient solution temperatures interacted to influence calculated concentrations of P, Ca, Mg, S, B, Cu, Mn, and Mo in dry shoot tissue (**Table 3, Fig. 2A-H**). In general, green basil accumulated greater shoot concentrations of P, Ca, S, B, Cu, Mn, and Mo as AT and NST increased; however, when grown in 30 °C AT, Mg, S, and Ca shoot concentrations decreased and then increased as NST increased. Overall, plants grown with 20 °C AT and 35 °C NST target setpoints accumulated the greatest concentrations of P, Ca, S, Mn, and Mo. Magnesium concentrations were greatest in plants grown with 30 °C AT and 15 °C NST target setpoints, B concentrations were greatest in plants grown with 30 °C AT and 35 °C NST target setpoints, and Cu concentrations were greatest in plants grown with 30 °C AT and 30 °C NST target setpoints.

Plants grown in 20 °C AT with 35 °C NST were calculated to accumulate 0.53% (5.3 $mg \cdot g^{-1}$) more P, 0.85% (8.5 $mg \cdot g^{-1}$) more Ca, 0.03% (0.3 $mg \cdot g^{-1}$) more S, 8.82% (88 $\mu g \cdot g^{-1}$) more B, 162% (11.5 $\mu g \cdot g^{-1}$) more Cu, 125.44% (97.7 $\mu g \cdot g^{-1}$) more Mn, and 447.28% (0.84 $\mu g \cdot g^{-1}$) more Mo, compared with those grown in 15 °C NST. Plants grown in 20 °C AT with 25 °C NST accumulated 0.01% (1.0 $mg \cdot g^{-1}$) more Mg, compared with those grown in 15 °C NST. Plants grown in 30 °C AT with 35 °C NST were calculated to accumulate 0.11% (11 $mg \cdot g^{-1}$) more P, 0.16% (16 $mg \cdot g^{-1}$) less Mg, 0.09% (9.2 $mg \cdot g^{-1}$) less S, 0.96 $\mu g \cdot g^{-1}$ more B, 4.54 $\mu g \cdot g^{-1}$ more Cu, and 20.3 $\mu g \cdot g^{-1}$ more Mn than those grown with 15 °C NST.

The calculated quadratic responses of N and K concentrations decreased and then increased as AT increased; the quadratic responses of N and K increased and plateaued as NST increased from 15 to 35 °C (**Fig. 3A-D**). Iron increased linearly and Zn increased quadratically as NST increased (**Table 3, Fig. 3E-F**). Plants grown in 30 °C AT were calculated to accumulate 1% (10 $mg \cdot g^{-1}$) more N and 2% (20 $mg \cdot g^{-1}$) more K than those grown in 20 °C AT. Likewise, plants grown in 35 °C NST were calculated to accumulate 1% (10 $mg \cdot g^{-1}$) greater N and 17.2 $\mu g \cdot g^{-1}$ more Fe, and those grown in 25 °C NST would accumulate 1% (10 $mg \cdot g^{-1}$) more K and 27.3 $\mu g \cdot g^{-1}$ more Zn, than those grown in 15 °C NST.

Basil 'Red Rubin'

Air and nutrient solution temperatures interacted to influence basil 'Red Rubin' FM, SDM, STDM, SH, and IL (**Table 2, Fig. 4A-F**). Basil 'Red Rubin' FM, SDM, STDM, SH, and IL. All parameters quadratically increased as AT increased from 20 to 30 °C and NST increased from 15 to 30 °C, then decreased in higher NSTs.

Basil ‘Nufar’

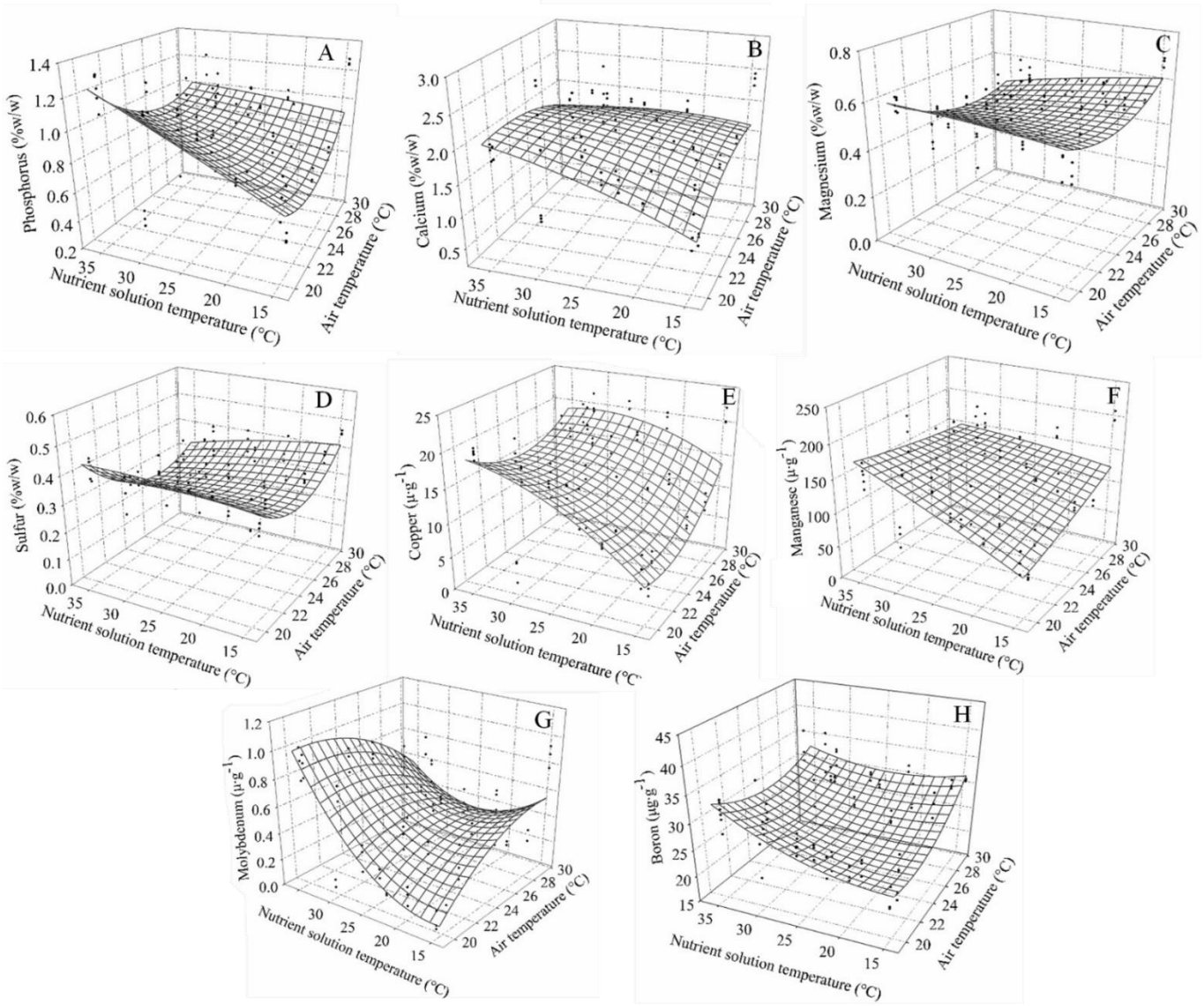


Figure 2. Basil (*Ocimum basilicum*) ‘Nufar air temperature and nutrient solution temperature interaction effects on dry shoot concentrations (percent dry mass or $\mu g \cdot g^{-1}$) of phosphorus (A), calcium (B), magnesium (C), sulfur (D), copper (E), manganese (F), and molybdenum (G).

Basil ‘Nufar’

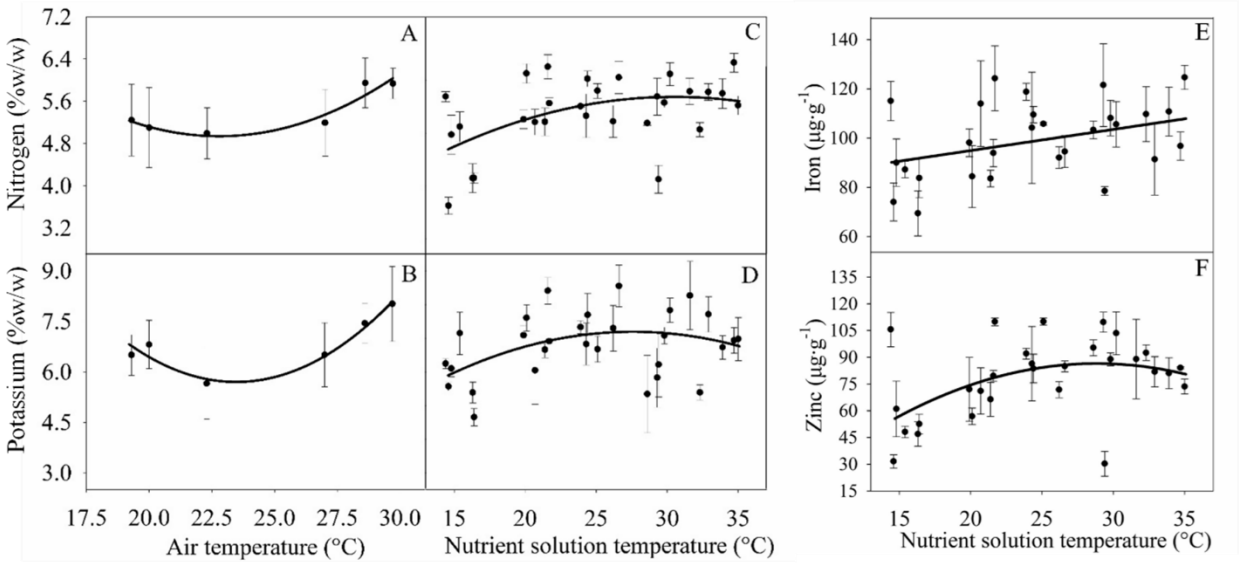


Figure 3. Air temperature influences on basil (*Ocimum basilicum*) ‘Nufar’ dry shoot concentrations (%w/w) of nitrogen (A) and potassium (B), as well as nutrient solution temperature influences on nitrogen (C), potassium (D), iron (E), and zinc (F) concentrations.

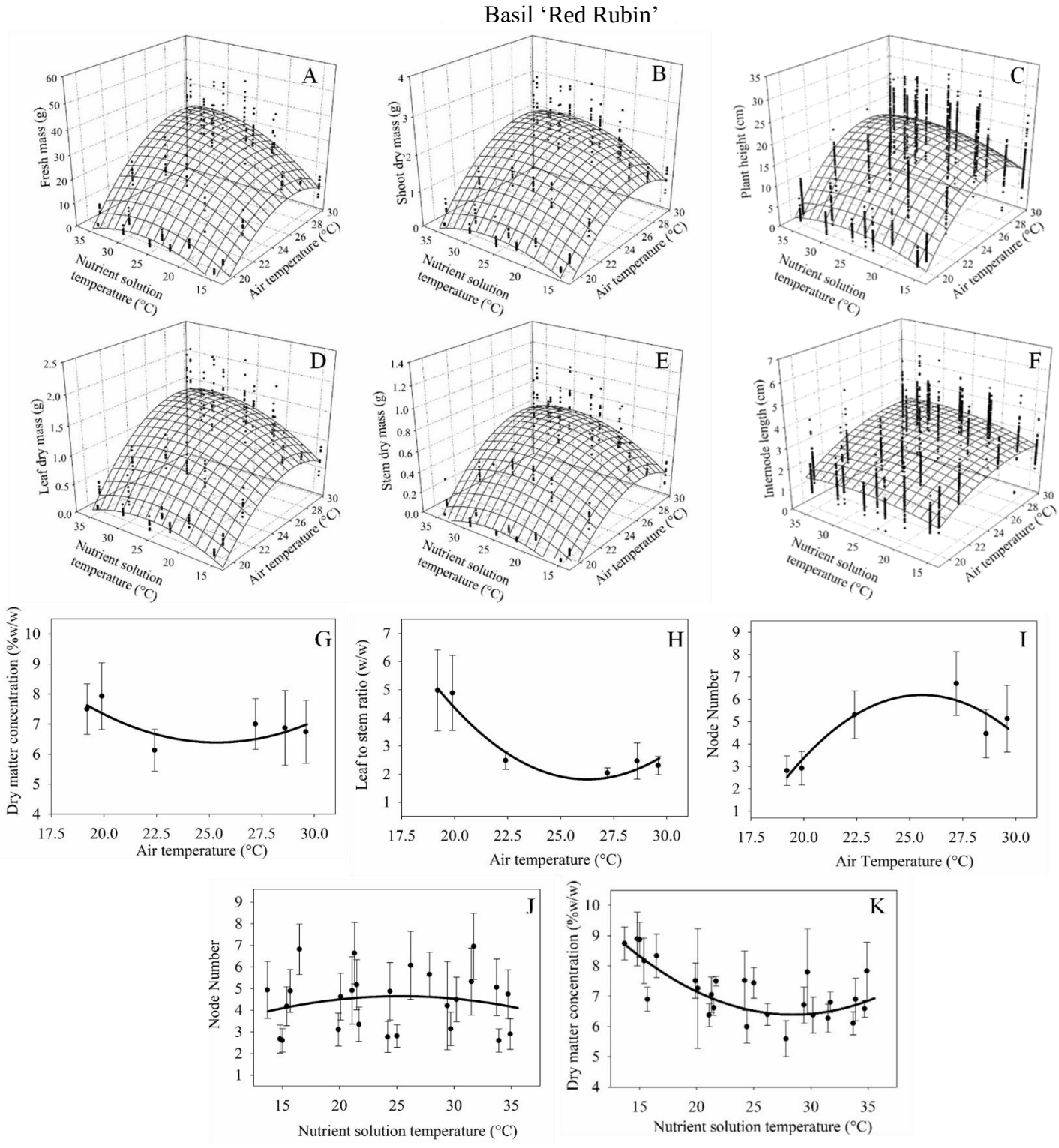


Figure 4. Basil (*Ocimum basilicum*) 'Red Rubin' air and nutrient solution temperature interaction effects on fresh mass (A), shoot dry mass (B), plant height (C), leaf dry mass (D), stem dry mass (E), internode length (F), air temperature influence on node number (G), leaf to stem ratio (H), dry matter concentration (I), and nutrient solution temperature influence on node number (J) and dry matter concentration (K).

Red basil grown in 20 °C AT with 25 °C NST were calculated to produce 286% (8.0 g) greater FM, 134% (0.43 g) more SDM, 94% (0.27 g) greater LDM, 491% (0.16 g) greater STDM, 41% (2.5 cm) greater SH, and 14% (0.9 cm) greater IL compared with those grown in 15 °C NST. In 30 °C AT, plants grown with 30 °C NST were calculated to produce 150% (18.8 g) greater FM, 90% (0.96 g) greater SDM, 83% (0.64 g) more LDM, 112% (0.32 g) more STDM, 43% (4.7 cm) greater SH, and 24% (0.6 cm) larger IL compared with those grown in 15 °C NST.

Air temperature influenced basil 'Red Rubin' DMC, LSR, and NN (**Table 2, Fig. 4G-I**). The quadratic responses of LSR and DMC decreased then plateaued, while NN increased and then bagan to decrease as AT increased from 20 to 30 °C. Basil 'Red Rubin' grown in 30 °C AT was calculated to produce 37% lower LSR, 11% lower DMC, and 31% greater NN compared with those grown in 20 °C AT.

Likewise, DMC quadratically decreased then increased, while NN quadratically increased then plateaued as NST increased from 15 to 30 °C (DMC) or 15 to 25 °C (NN) (**Table 2, Fig. 4J and K**). Red basil grown in 30 °C NST had a calculated 21% lower DMC, and plants grown in 25 °C NST produced 11% greater NN than those grown in 15 °C NST.

Air and nutrient solution temperatures interacted to influence dry shoot concentrations of Ca, Mg, B, Fe, and Mo (**Table 3, Fig. 5A-E**). Basil 'Red Rubin' shoot concentrations of Mg and B quadratically decreased then increased with increasing NST and AT. Concentrations of Fe and Mo quadratically increased with increasing NST, and quadratically decreased then increased with increasing AT. Calcium concentrations quadratically increased then decreased with increasing AT and NST. Plants accumulated the greatest concentrations of Ca with 20 °C AT and 30 °C NST, the greatest concentration of Mg in 30 °C AT and 15 °C NST, and the greatest concentrations of B, Mo, and Fe in 20 °C AT and 35 °C NST.

Plants grown in 20 °C AT with 35 °C NST were calculated to accumulate 8.1 $\mu g \cdot g^{-1}$ more B, 78.3 $\mu g \cdot g^{-1}$ more Fe, and 0.6 $\mu g \cdot g^{-1}$ more Mo than those grown in 15 °C NST, and plants grown with 30 °C NST were calculated to accumulate 0.14% (1.4 $mg \cdot g^{-1}$) more Ca and 0.03% (0.3 $mg \cdot g^{-1}$) more Mg than those grown in 15 °C NST. In 30 °C AT, plants grown with 35 °C NST accumulated 0.19% (1.9 $mg \cdot g^{-1}$) more Ca, 0.14% (1.4 $mg \cdot g^{-1}$) less Mg, 1.6 $\mu g \cdot g^{-1}$ less Fe, and 0.3 $\mu g \cdot g^{-1}$ more Mo, and plants grown in 25 °C NST accumulated 5.9 $\mu g \cdot g^{-1}$ less B compared with those grown in 15 °C NST.

Basil ‘Red Rubin’

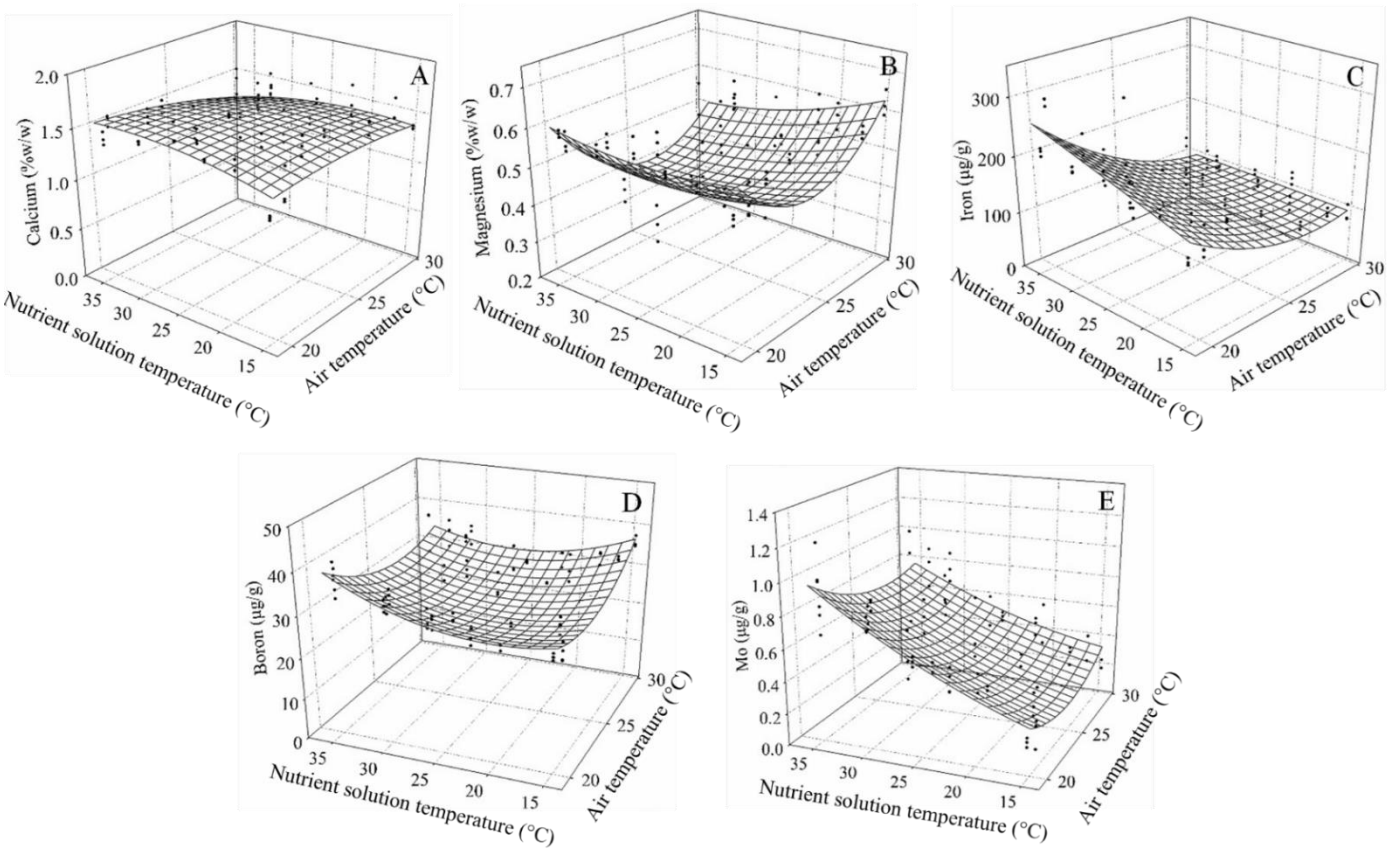


Figure 5. Basil (*Ocimum basilicum*) ‘Red Rubin’ air temperature and nutrient solution temperature interaction effects on shoot concentrations of calcium (A), magnesium (B), iron (C), boron (D), and molybdenum (E).

Air and nutrient solution temperatures influenced concentrations of K, S, Cu, Mn, and Zn, while only AT influenced P and only NST influenced N (**Table 3, Fig. 6A-L**). Basil 'Red Rubin' shoot concentrations of P, K, S, Cu and Mn quadratically decreased, then increased, as AT increased from 20 to 30 °C; however, shoot Zn concentrations increased and then decreased as AT increased from 20 to 30 °C. Shoot concentrations of K and Mn linearly increased as NST increased from 15 to 35 °C; Zn, Cu, and N concentrations quadratically increased as NST increased from 15 to 30 °C; and S and P concentrations quadratically decreased then increased as NST increased from 15 to 30 °C.

Plants grown in 30 °C AT were calculated to accumulate 0.05% (0.5 $mg \cdot g^{-1}$) more P, 1.6% (16 $mg \cdot g^{-1}$) more K, 0.03% (0.3 $mg \cdot g^{-1}$) less S, 1.9 $\mu g \cdot g^{-1}$ more Cu, 4.8 $\mu g \cdot g^{-1}$ less Mn, and 29.8 $\mu g \cdot g^{-1}$ less Zn than those grown in 20 °C AT. Plants grown in 35 °C NST were calculated to accumulate 0.64% (6.4 $mg \cdot g^{-1}$) more K, 0.04% (0.4 $mg \cdot g^{-1}$) less S, 9.32 $\mu g \cdot g^{-1}$ more Cu, 28.34 $\mu g \cdot g^{-1}$ more Mn, 51.8 $\mu g \cdot g^{-1}$ more Zn, and 0.65% (6.5 $mg \cdot g^{-1}$) more N than those grown in 15 °C NST.

Cilantro 'Santo'

Air and nutrient solution temperatures interacted to influence cilantro 'Santo' DMC and plant length (PL). In general, PL quadratically increased as AT and NST increased, up to a maximum in 30 °C AT with 20 °C NST. However, DMC quadratically decreased, then increased as AT and NST increased, with the highest DMC in plants grown at 30 °C AT and 35 °C NST.

At 20 °C AT, cilantro 'Santo' grown with 25 °C NST was calculated to produce 23% (6.9 cm) greater PL than those grown in 15 °C NST, while those grown in 35 °C NST produced 49% greater DMC compared with 15 °C NST (**Table 2, Fig. 7A-B**) 30 °C AT, plants grown with 20 °C NST were calculated to produce 12% (4.5 cm) greater PL compared to those grown in 15 °C and produce 85% greater DMC with 35 °C NST than those in 15 °C NST.

Nutrient solution temperatures significantly influenced cilantro 'Santo' FM and DM, while NST and AT influenced leaf number (LN) (**Table 2, Fig. 7C-E**). Cilantro FM, DM, and LN quadratically increased as NST increased from 15 to 25 °C, then decreased in higher NSTs; likewise, LN quadratically increased from 20 to 30 °C AT, though the response was modest.

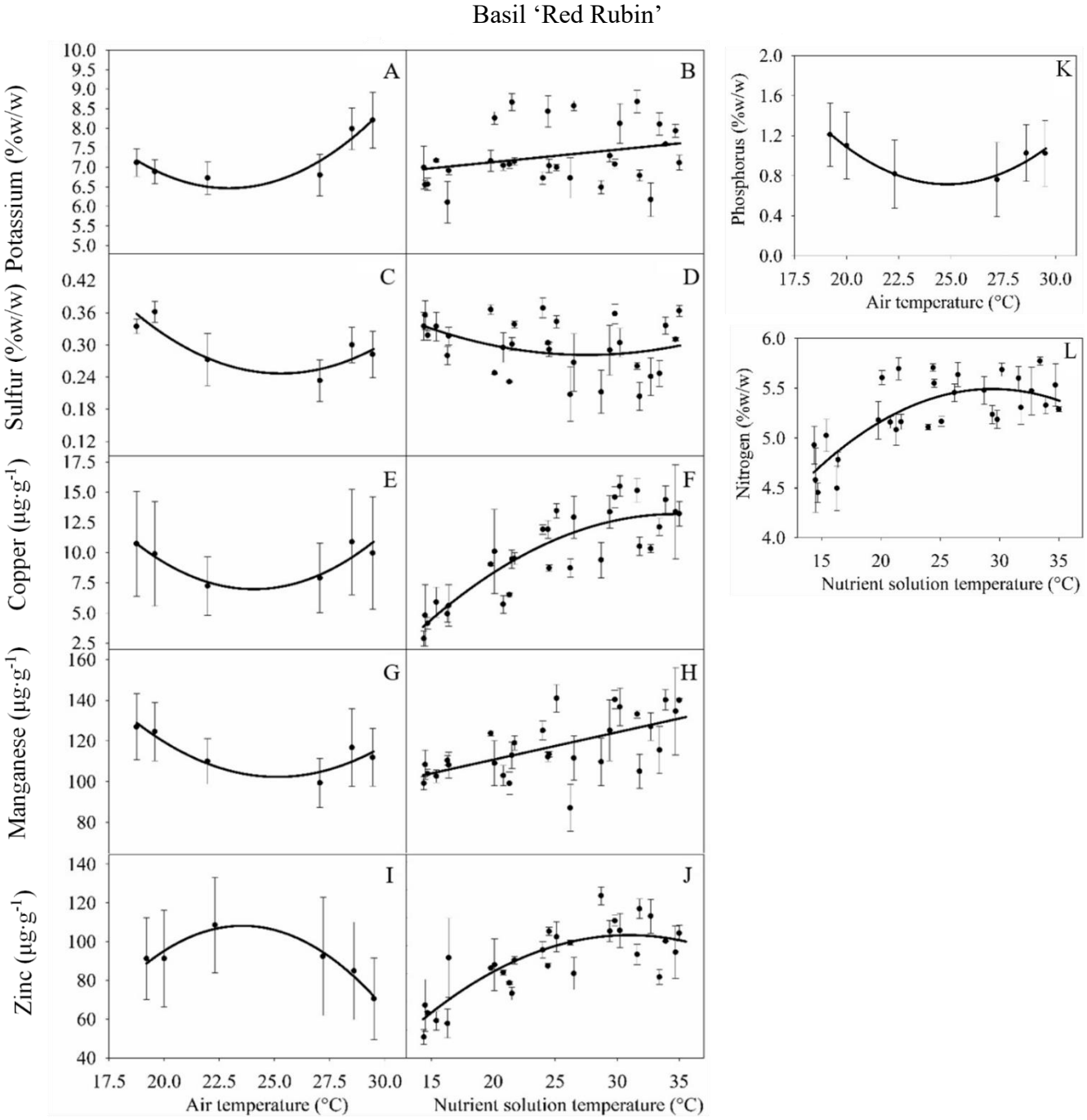


Figure 6. Air temperature effects on basil (*Ocimum basilicum*) ‘Red Rubin’ dry shoot concentrations of potassium (A), sulfur (C), copper (E), manganese (G), zinc (I), and phosphorus (K); as well as nutrient solution temperature effects on potassium (B), sulfur (D), copper (F), manganese (H), zinc (J), and nitrogen (L).

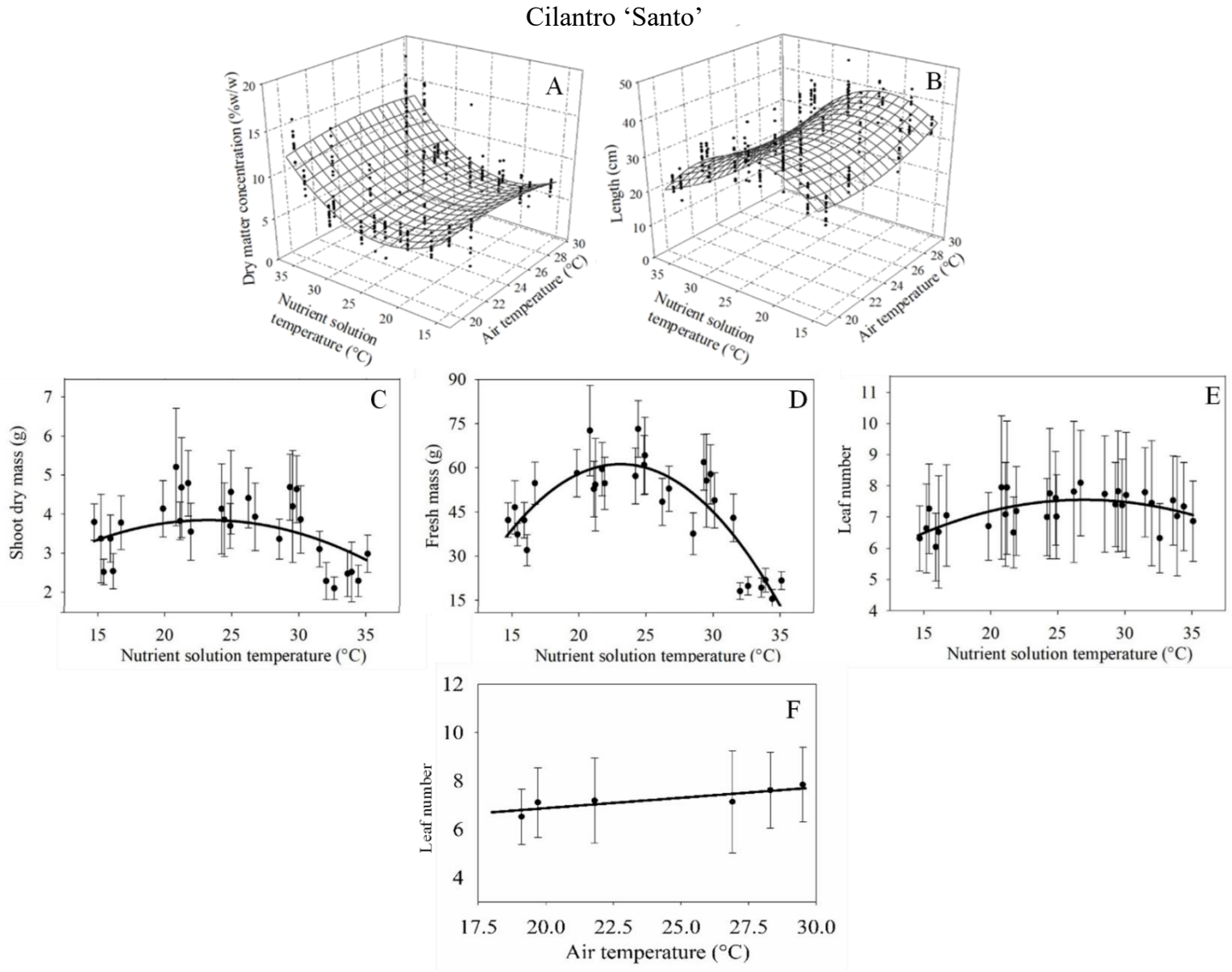


Figure 7. Air and nutrient solution temperature interaction effects on cilantro (*Coriandrum sativum*) ‘Santo’ dry matter concentration (A) and plant length (B), air temperature effects on leaf number (F), and nutrient solution temperature effects on shoot dry mass (C), fresh mass (D), and leaf number (E)

Cilantro ‘Santo’ grown with 25 °C NST was calculated to produce 58% (20.90 g) greater FM, 41% (1.17 g) greater DM, and 16% (0.7) larger LN compared with those grown in 15 °C NST. Likewise, cilantro grown in 30 °C AT were calculated to produce 9% (0.6) greater LN than those grown in 20 °C AT.

Air and nutrient solution temperatures interacted to influence shoot tissue concentrations of K and Cu (**Table 3, Fig. 8A-B**). Shoot K and Cu concentrations quadratically decreased then increased as AT increased to 30 °C, and K concentrations quadratically increased as NST increased to 20 °C, and Cu concentrations quadratically increased as NST increased to 25 °C. Overall, plants grown in 30 °C AT and 20 °C NST would accumulate the highest K concentrations, and plants grown in 30 °C AT and 25 °C NST would accumulate the highest Cu concentrations.

Plants grown in 20 °C AT with 35 °C NST were calculated to accumulated 2.14% (21.4 $mg \cdot g^{-1}$) less K and 3.05 $\mu g \cdot g^{-1}$ more Cu than those grown with 15 °C NST. Plants grown in 30 °C AT with 20 °C NST were calculated to accumulate 4.1% (41.0 $mg \cdot g^{-1}$) more K compared with those grown in 35 °C NST, and those grown with 25 °C NST accumulated 4.48 $\mu g \cdot g^{-1}$ more Cu than those grown in 15 °C NST.

Air and nutrient solution temperatures influenced concentrations of N, P, S, B, Fe, Mn, and Zn while only NST influenced Ca, Mg, and Mo (**Table 3, Fig. 9A-M, Fig. 10A-D**). Cilantro accumulated greater amounts of N, P, Mn, Mo, and Zn and less S, B, Fe when grown in 30 °C AT compared to 20 °C AT.

Cilantro shoot concentrations of Mg, S, and Fe linearly decreased as NST increased from 15 to 35 °C; concentrations of N and P quadratically decreased with NST up to 20 °C, then increased as NST increased to 35 °C; and concentrations of Zn, Mn, and Ca quadratically increased with NST up to 25 °C, then declined in 30 and 35 °C NST.

Plants grown in 30 °C AT were calculated to accumulate 0.62% (6.3 $mg \cdot g^{-1}$) greater N, 0.04% (0.4 $mg \cdot g^{-1}$) more P, 0.05% (0.5 $mg \cdot g^{-1}$) less S, 1.4 $\mu g \cdot g^{-1}$ less B, 12.2 $\mu g \cdot g^{-1}$ less Fe, 17.9 $\mu g \cdot g^{-1}$ more Mn, and 9.0 $\mu g \cdot g^{-1}$ more Zn than those grown in 20 °C AT. Plants grown in 35 °C NST would accumulate 2.05% (20.5 $mg \cdot g^{-1}$) less N, 0.42% (4.2 $mg \cdot g^{-1}$) less P, 0.052% (0.52 $mg \cdot g^{-1}$) more Mg, 0.11% (1.1 $mg \cdot g^{-1}$) less S, 16.1 $\mu g \cdot g^{-1}$ more B, and 42.1 $\mu g \cdot g^{-1}$ less Fe than

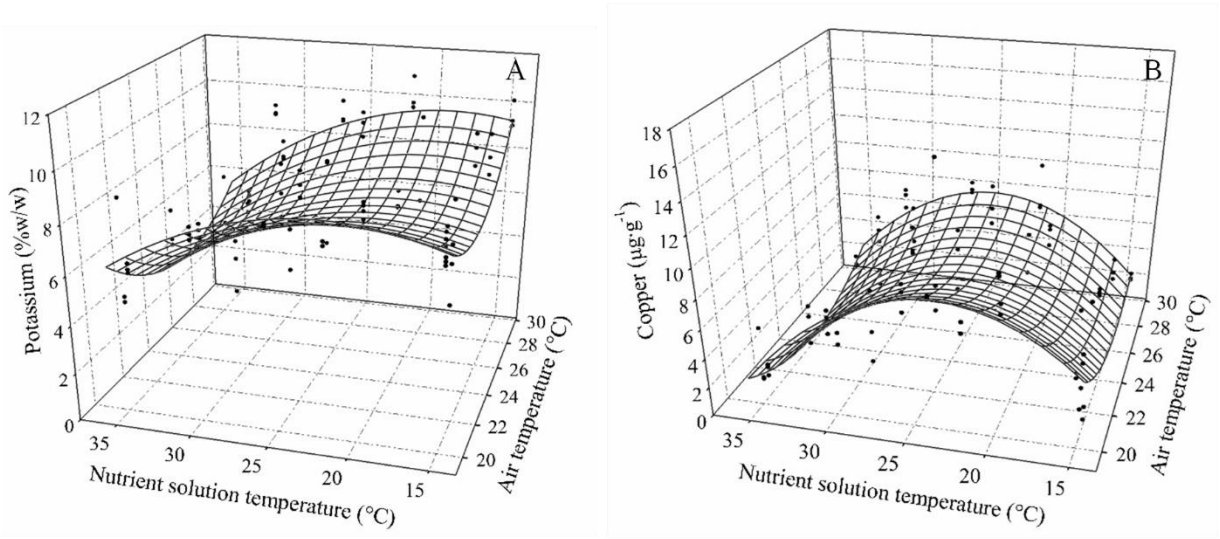


Figure 8. Air and nutrient solution temperature interaction effects on cilantro (*Coriandrum sativum*) ‘Santo’ shoot concentrations of potassium (A) and copper (B).

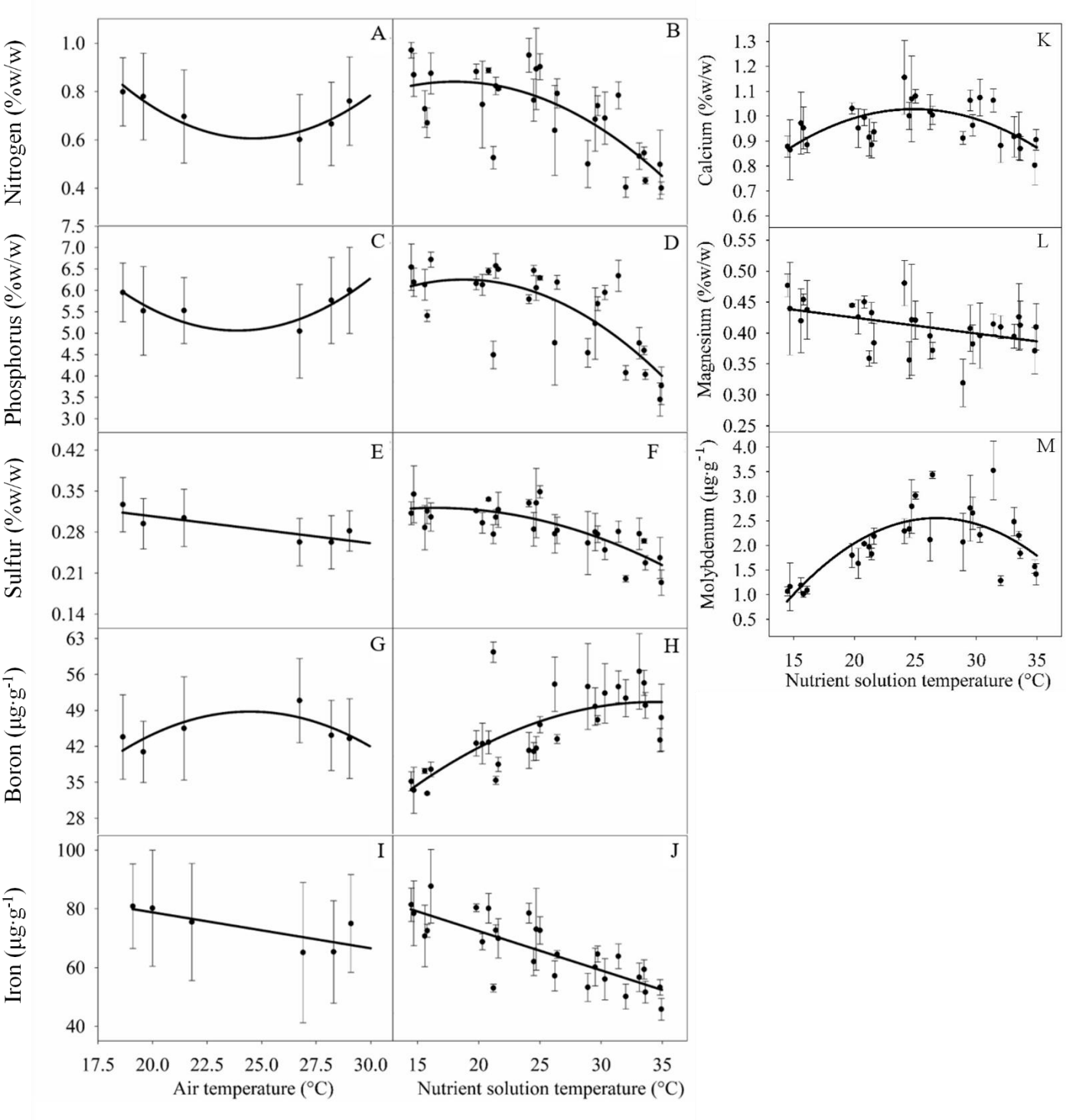


Figure 9. Air temperature effects on cilantro (*Coriandrum sativum*) ‘Santo’ dry shoot concentrations of nitrogen (A), phosphorus (C), sulfur (E), boron (G), and iron (I); as well as nutrient solution temperature effects on nitrogen (B), phosphorus (D), sulfur (F), boron (H), iron (J), calcium (K), magnesium (L), and molybdenum (M).

Cilantro ‘Santo’

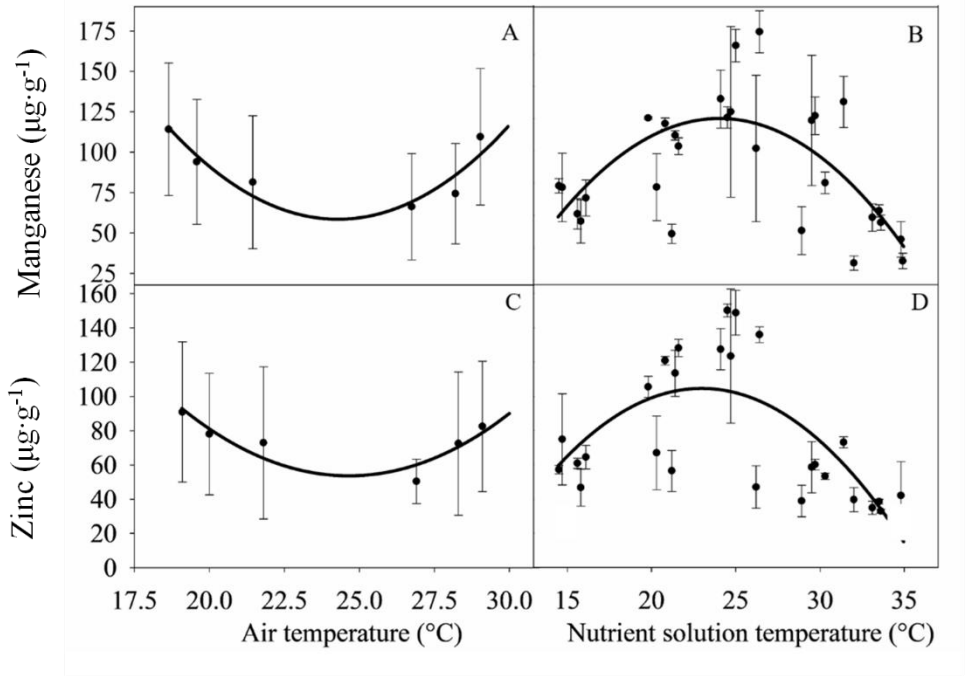


Figure 10. Air temperature influence on cilantro (*Coriandrum sativum*) ‘Santo’ manganese (A) and zinc (B), as well as nutrient solution temperature influence on manganese (C) and zinc (D).

those grown in 15 °C NST, while plants grown in 25 °C NST would accumulate 0.152% (1.52 $mg \cdot g^{-1}$) more Ca, 53.6 $\mu g \cdot g^{-1}$ more Mn, and 37.0 $\mu g \cdot g^{-1}$ more Zn than those grown in 15 °C NST.

Cilantro shoot concentrations of Mg, S, and Fe linearly decreased as NST increased from 15 to 35 °C; concentrations of N and P quadratically decreased with NST up to 20 °C, then increased as NST increased to 35 °C; and concentrations of Zn, Mn, and Ca quadratically increased with NST up to 25 °C, then declined in 30 and 35 °C NST.

Plants grown in 30 °C AT were calculated to accumulate 0.62% (6.3 $mg \cdot g^{-1}$) greater N, 0.04% (0.4 $mg \cdot g^{-1}$) more P, 0.05% (0.5 $mg \cdot g^{-1}$) less S, 1.4 $\mu g \cdot g^{-1}$ less B, 12.2 $\mu g \cdot g^{-1}$ less Fe, 17.9 $\mu g \cdot g^{-1}$ more Mn, and 9.0 $\mu g \cdot g^{-1}$ more Zn than those grown in 20 °C AT. Plants grown in 35 °C NST would accumulate 2.05% (20.5 $mg \cdot g^{-1}$) less N, 0.42% (4.2 $mg \cdot g^{-1}$) less P, 0.052% (0.52 $mg \cdot g^{-1}$) more Mg, 0.11% (1.1 $mg \cdot g^{-1}$) less S, 16.1 $\mu g \cdot g^{-1}$ more B, and 42.1 $\mu g \cdot g^{-1}$ less Fe than those grown in 15 °C NST, while plants grown in 25 °C NST would accumulate 0.152% (1.52 $mg \cdot g^{-1}$) more Ca, 53.6 $\mu g \cdot g^{-1}$ more Mn, and 37.0 $\mu g \cdot g^{-1}$ more Zn than those grown in 15 °C NST.

Common sage

Nutrient solution temperature influenced FM, SH, and NN in sage (**Table 2, Fig. 11A-C**). Sage FM, NN, and SH quadratically increased as NSTs increased from 15 to 20 °C (SH) or 25 °C (FM, NN), then declined in higher NSTs. Plants grown with 20 °C NST were calculated to yield 6% (0.8 cm) greater SH, and those grown in 25 °C NST were calculated to yield 67% (13.7 g) greater FM and 3% greater NN than plants grown with 15 °C NST (Table 2).

Parsley 'Giant of Italy'

Nutrient solution temperature influenced FM, PH, and LN (**Table 2, Fig. 12A-C**). Parsley FM, PH, and LN quadratically increased as NST increased from 15 to 25 °C, then decreased in NSTs above 25 °C. Plants grown in 25 °C NST were calculated to yield 64% (16.0 g) greater FM, 25% (6.4 cm) greater PH, and 11% greater LN than those grown in 15 °C NST.

Discussion

Basil 'Nufar' and 'Red Rubin' grew longer stems and internodes, produced more nodes, and yielded more fresh and dry mass as AT and NST increased. Overall, plants grown in 30 °C, plants grown in 30 °C AT with 30 °C NST target setpoints produced the greatest FM, SDM, LDM, STDM, SH, IL, and NN (Table 2, Fig. 1A-H, 2A-H).

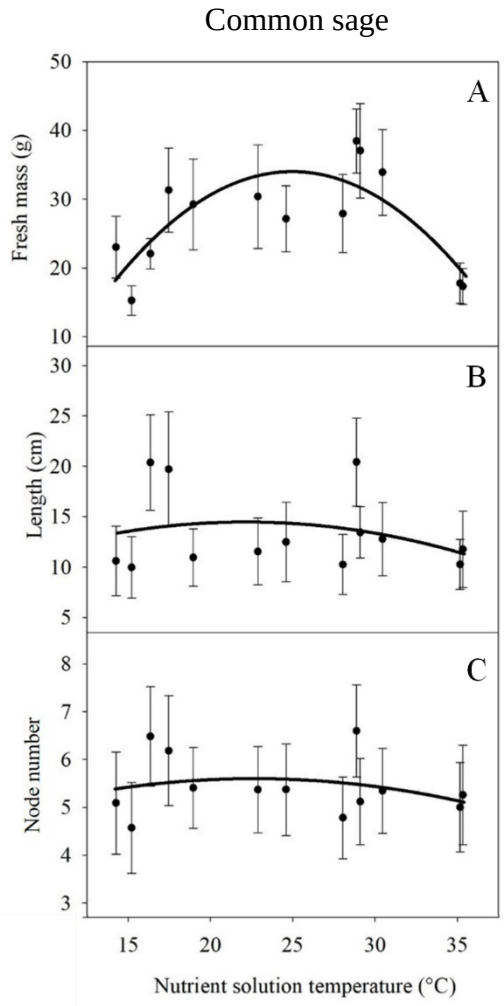


Figure 11. Nutrient solution temperature effects on common sage (*Salvia officinalis*) fresh mass (A), plant length (B), and node number (C).

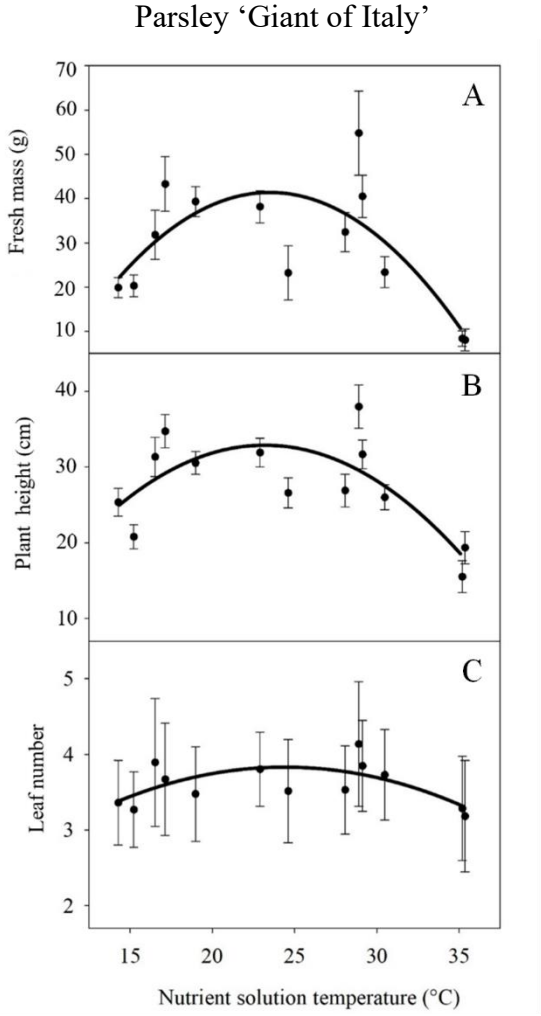


Figure 12. Nutrient solution temperature effects on parsley (*Petroselenium crispum*) ‘Giant of Italy’ fresh mass (A), plant height (B), and leaf number (C).

This agrees with previous work which reported ≈30 °C as the optimal AT for basil yield (Al-Huqail et al., 2020; Barickman et al., 2021; Fallahi, 2015; Hendrickson et al., 2022; Walters and Currey, 2019). Hendrickson et al. (2022) grew basil in temperature controlled nutrient reservoirs (27.5 or 31 °C) and found that FM, DM, SH, and shoot N concentrations increased compared with those grown in 23 °C NST. In temperatures of ≈32 ºC and higher, basil LN, SL, and FM yields have been reported to decline relative to temperatures ranging from 25 to 30 ºC, which also agrees with our observed trends (Al-Huqail et al., 2020; Barickman et al., 2021).

Dry matter concentration and LSR in both basil cultivars declined as AT and NST increased. Chang et al. (2005) compared basil grown in 15, 25, and 30 °C AT, and found that those grown in 15 °C AT yielded less fresh mass, dry mass, nodes, and water content (WC). This is consistent with our results, given that WC is the inverse of our DMC calculation.

Bryson et al. (2014) established the following tissue sufficiency ranges for mineral concentrations in basil leaves, which will be the referenced values throughout the remaining results: 3.5-5.5% N, 1-3% P, 1.55-2.05% K, 1.25-2.00% Ca, 0.6-1.25% Mg, 0.2-0.6% S, 25-60 $\mu g \cdot g^{-1}$ B, 5-10 $\mu g \cdot g^{-1}$ Cu, 75-200 $\mu g \cdot g^{-1}$ Fe, 30-150 $\mu g \cdot g^{-1}$ Mn, and 30-70 $\mu g \cdot g^{-1}$ Zn. Basil ‘Nufar’ and ‘Red Rubin’ shoot concentrations of most mineral nutrients fell within those ranges, with some exceptions, and all mineral nutrients were influenced by at least AT or NST. Our results do not fully align with Hendrickson et al. (2022), who described effects of NST only on N, Cu, and Mn tissue concentrations, however they utilized fewer NST treatments (23, 27, and 31 °C) and analyzed leaf instead of whole shoot tissue.

Shoot concentrations of N in Basil ‘Nufar’ and ‘Red Rubin’ were all within or slightly above the sufficiency range. Basil ‘Nufar’ accumulated greater concentrations of N as AT and NST increased, while basil ‘Red Rubin’ shoot N concentrations were not influenced by AT but did increase as NST increased. Increasing shoot N concentrations with increasing NST and AT agrees with some previous work (Hendrickson et al., 2022; Solis-Toapanta et al., 2020). Basil ‘Nufar’ and ‘Red Rubin’ accumulated excess K across all treatment combinations. Additionally, K concentrations increased with increasing AT and NST. Even the basil treatment with the lowest shoot K concentrations accumulated ≈3 times more K than the recommended upper limit of the sufficiency range, which could indicate luxury uptake of K. Shoot Ca concentrations in basil ‘Nufar’ grown in 20 °C AT with 35 °C NST slightly exceeded the sufficiency range, while basil ‘Red Rubin’ grown in 30 °C AT with 35 °C NST was slightly deficient; plants grown in all

remaining treatment combinations had Ca concentrations within the recommended sufficiency range. Basil 'Nufar' and 'Red Rubin' Ca concentrations increased as NST increased when grown in 20 °C AT; on the other hand, basil 'Red Rubin' grown in 30 °C AT exhibited a decrease in Ca concentration as NST increased from 15 to 35 °C and basil 'Nufar' exhibited a decrease in Ca concentration as NST increased beyond 25 °C. With the exception of basil 'Nufar' grown in 30°C AT with 15 °C NST and basil 'Red Rubin' grown in 30 °C AT with 15, 20, or 25 °C NST, all plants accumulated Mg concentrations slightly below the recommended sufficiency range. Shoot Mg concentrations declined with increasing NST in 30 °C AT, while in 20 °C AT shoot Mg concentrations slightly increased as NST increased from 15 to 25 °C, then decreased in higher NSTs. High tissue K concentrations have been associated with decreased Mg and Ca concentrations (Dibb and Thompson, 1985; Walters and Currey, 2018), and the luxury K uptake observed in this study may have antagonized uptake of Mg and Ca at elevated AT and NSTs. Aside from antagonism, shoot concentrations of mineral nutrients may appear suppressed in higher temperatures due to a "dilution" effect, wherein the biomass outpaces any difference in mineral accretion by those tissues under those treatments, and thus the proportion of mineral nutrients to organic tissue (predominantly carbon, oxygen, and hydrogen by mass) is lower. While shoot S concentrations in basil 'Nufar' and 'Red Rubin' fell within the recommended tissue sufficiency range, S concentrations in basil 'Nufar' grown in 20 °C AT increase as NST increased from 15 to 35 °C, decreased in basil 'Nufar' grown in 30 °C AT as NST increased, and decreased in basil 'Red Rubin' at both ATs as NST increased.

Given our findings and those of other researchers, controlled environment producers who wish to grow basil should consider the following: basil fresh mass yield is highly responsive to AT, with ≈30 °C as the T_{opt} for many cultivars, so prioritize AT above NST; however, NST cooling to 28 ± 2 °C can enhance yield in ≈30 °C AT. If ≈30 °C AT is untenable, NST heating up to 28 ± 2 °C may greatly improve basil biomass yield at suboptimal (< 28 ±2 °C) ATs. Cooling the NST by 0-5 °C (compared to air ADT) improved biomass yield at ATs of 28 ±2 °C, while heating NST by 5 °C (compared to air ADT) improved biomass yield at ATs of 20 ±2 °C.

Day-night temperature differences (DIF), calculated as the mean temperature (photoperiod) – mean temperature (dark period), are common in greenhouse production. Higher day temperatures compared to night temperatures produces a positive DIF, while higher night temperatures compared with day temperatures produces a negative DIF. In basil, compared with

a static temperature regime, positive DIFs may improve fresh mass yield, plant length, and node number, while negative DIFs often result in shorter stems with lower biomass yield (Frąszczak et al., 2011; Islam et al., 2016). Heating a nutrient solution above ambient temperatures in a static fashion (minimal diurnal fluctuation) may partially reduce the influence of a positive AT DIF setting by elevating nocturnal root respiration or altering ion uptake kinetics (Peraudeau et al., 2015). A potential indicator parameter of this phenomenon is DMC because it indirectly informs us about photosynthate partitioning and tissue hydration. The decrease in DMC that we observed in basil as NST increased could indicate a concomitant rise in nocturnal respiration, greater water and ion transport or retention, or a combination of those factors.

Barickman et al. (2021) grew basil 'Genovese' in low (20/12 day/night), control (30/22), and high (38/30) °C AT, and found that net photosynthesis, stomatal conductance to water vapor, and electron transport rate were highest in plants grown in 38/30 °C AT. Frąszczak et al. (2011) found that basil grown in a +5 °C DIF for 14 d yielded ≈2-fold FM and ≈15% greater SH than those grown with a -5 or 0 °C DIF, despite all treatments providing 23 °C average daily temperatures (ADTs). Positive DIFs can benefit basil growth and yield, and it is difficult to rule out the possibility that our NST treatments negated the benefit of the AT DIF which we imposed, by heating some of the root-zones during the night. For example, basil growth in 30 °C AT was better with 25 °C NST than with 15 °C NST, which could be due to a greater impact of temperature in slowing root development and mineral exchange at the root-solution interface in this cold-sensitive species which overshadowed the benefit of decreased photosynthate losses due to lower root respiration. However, root fresh weight and root respiration were not measured in this study, so this could not be confirmed.

Cilantro 'Santo' FM, SDM, and LN were greatest in 25 °C NST, but insignificantly responded to AT. In NST beyond 25 °C, FM, SDM, and LN declined; FM yield was especially impaired temperatures of 30 °C or higher, whereas SDM and LN declined more modestly. Though previous researchers have described myriad AT responses in cilantro, the difference between the ATs which we provided may have been too narrow to significantly influence FM, SDM, and LN (Hückstädt et al., 2013; Mortensen et al., 2014). Additionally, the greenhouse bays were located side-by-side in an east-west orientation and therefore, the DLIs between them differed by up to 3 $mol \cdot m^{-2} \cdot d^{-1}$ despite attempts to change supplemental lighting thresholds throughout the seasons to account for that directional effect, which could possibly be a

confounding factor (Table 1). Regardless, the improved FM, DM, and SL in 25 °C NST compared with 15, 20, 30, and 35 °C NST agree with previous observations. Nguyen et al. (2020) grew cilantro transplants for 3 or 6 d with 15, 20, 25 (control), 30, or 35 °C NST; plants grown in 35 °C NST for 6 d and 15 °C NST for 3 d produced less FM and SL compared with the control. Additionally, Nguyen et al. (2019) grew cilantro in 20, 25, and 30 °C NST for 18 d, and found that plants grown in 20 and 30 °C NST produced less FM, DM, and lower WC compared with 25 °C NST. Thus, our finding that DMCs were greatest in low (15 °C) and high (30, 35 °C) NSTs agrees with previous research.

The optimum of 25 °C NST for parsley growth in 20 °C AT roughly aligns with previous work. Eidsten and Giselrod (1986) reported an optimal AT of 21 °C for yield and height, but found that plants grown in 18 °C AT with 24 °C NST produced 13% or 83% greater SL and 22% or 127% more SDM than those grown in 18 or 36 °C NST. Substituting 18 °C for AT and 24 °C for NST into our surface regression models to apply conditions similar to theirs would lead to 248% or 71% taller shoots and 19% or 276% greater fresh mass compared with those grown in 21 °C AT with 18 or 35 °C NST. This is a greater difference than their results; however, the substitution may have a higher error as we did not use 18 °C AT, and the trend (increase up to around 25 °C NST) is similar.

Sage produced the greatest FM and NN in 25 °C NST and the greatest PH in 20 °C. Previous studies demonstrated an AT T_{opt} of ≈25 °C for sage yield, PH, and NN, which could be a rough proxy for NST responses (Ghorbani and Esmaeilizadeh, 2017; Mortensen, 2014; Walters and Lopez, 2023). Natarajan et al. (2005) found that *Salvia splendens* were shorter, had thicker stems, greater dry mass, and scored higher on market ratings when exposed to 35 °C AT for 6 $h \cdot week^{-1}$ (for 3 weeks), then transferred to 30 or 35 °C AT, compared to those which grew in 30 °C AT without 35 °C preconditioning. Likewise, in our study, SH was reduced in 35 °C NST when compared to 30 °C NST.

Conclusion

In summary, producers growing basil ‘Nufar’ or ‘Red Rubin’ with a +5 DIF could regulate NST to achieve 25 °C, in 20 or 30 °C AT for the best combination of growth and development. For cilantro producers, AT of 25 ± 2 °C AT with 23 ± 2 °C NST was ideal for biomass yield and length. When AT exceeds the recommended optimum (25 ± 2 °C), NST cooling to 23 ± 2 °C may improve biomass yields, while NST heating in low AT (19 ± 1) °C

could also improve biomass yields. Producers who wish to grow common sage and parsley ‘Giant of Italy’ in ATs of 21 ± 2 °C should consider heating the NST up to 25 ± 2 °C as a viable option to improve FM, PH, NN, and LN. The interaction effect of AT and DIF with NST remains to be characterized, and research exploring those potential interactions, along with DLI, nutrient solution concentrations, or biostimulant application in tandem with NST treatments, could better inform producers. Likewise, we did not measure the energy efficiency of our NST treatments or the AT controls; as a result, it is difficult to make specific recommendations based on the relative energy consumption.

Chapter III:

Pre-harvest Air and Nutrient Solution Temperature Influence Basil Postharvest Longevity

Keywords: cold storage, culinary herbs

Abstract

Culinary herbs are high value specialty crops, which possess optimal flavor and aroma as fresh cut tissue. Refrigerated shipment and storage are the leading postharvest strategies to extend the shelf life of many fresh produce commodities, including herbs. Despite the benefits of refrigeration, herbs such as basil are cold sensitive and quickly deteriorate in temperatures below 12 °C. Storage temperatures above 12 °C, though, promote pathogen colonization and rapid water loss. Aside from post-harvest conditions, the pre-harvest environment can influence the shelf life of produce. Exposure to low or high temperatures can induce acquired thermal tolerance in plants. Thus, temperature control regimes may be a promising way to combine yield improvement, ideal morphology, as well as shelf-life extension. Therefore, the research objective was to quantify the effect of pre-harvest air and nutrient solution temperature on water loss of basil in post-harvest storage temperatures. We grew basil (*Ocimum basilicum*) 'Nufar' and 'Red Rubin' in 20 or 30 °C air temperature, using hydroponic deep-water-culture tanks with 15, 20, 25, 30, or 35 °C nutrient solution temperatures. After each replication, we collected fresh tissue samples, enclosed them in plastic containers, and stored them in 4 and 10 °C walk in coolers. Basil 'Nufar' and 'Red Rubin' lost water at a slower rate over a 12-day storage period as pre-harvest AT and NST increased. Basil 'Nufar' (green) lost nearly twice the amount of water by weight in comparison with 'Red Rubin' (red), possibly due to its greater leaf size, or lower cold tolerance.

Introduction

Culinary herbs are specialty crops used in cooking, essential oil production, and cosmetic products. Herbs are important for those applications due to their variety of flavor and aroma profiles, provided by a litany of volatile organic compounds.

Herb flavors and aromas are most pronounced in fresh tissue, but drying extends shelf life (Prusinowska and Śmigielski, 2015). Following harvest, fresh herb tissue faces mechanical damage, temperature stress, and microbial colonization and degradation, all of which greatly reduce herb quality and salability (Loaiza and Cantwell, 1997). Practices such as refrigeration, rapid transit, and sanitary storage and handling procedures can extend fresh herb quality; however, cold-sensitive species degrade rapidly in refrigeration (Aharoni et al., 2010). Basil (*Ocimum basilicum*) is the most popular culinary herb species and grows best in air temperatures

around 30 °C with a nutrient solution temperature around 20 to 25 °C (Al-Huqail et al., 2020; Barickman et al., 2021; Fallahi, 2015; Hendrickson et al., 2022; Walters and Currey, 2019). Temperatures around or below 12 °C halt basil growth and induce wilting, browning, and lesions (Lange and Cameron, 1994; Wongsheree et al., 2009). Common methods to reduce chilling stress in basil storage include specialized packaging, higher temperature storage and shipment, and sale of potted plants instead of cut shoots; however, those solutions require extra input costs. An alternative route to improve basil shelf life in chilled storage would be to modify pre-harvest growth conditions.

Pre-harvest conditions such as air temperature could influence basil storage and decay. Lange and Cameron (1994) found that pre-harvest conditioning in 10 °C AT improved basil shelf life in cold storage compared to unconditioned plants, but conditioning at lower temperature (7.5 °C AT) accelerated the development chilling injury (CI) in storage. Aharoni et al. (2010) heated basil plants to 38 °C for 4 hours directly after harvest and observed reduced CI in 9 °C storage compared to those without heat treatment and attributed the difference to a surge in heat shock protein accumulation and possible surface disinfestation. Given the influence of pre-harvest conditions on post-harvest longevity, the research objective was to quantify the effect of pre-harvest air and nutrient solution temperature on water loss of basil in post-harvest storage temperatures.

Materials and methods

Growing conditions

Basil ‘Nufar’ and ‘Red Rubin’ were grown concurrently with the experimental plants in Chapter 2. Please see the Chapter 2 methods section for more details.

Data collection

Ten cells from each treatment were divided into 30 ± 2 g portions of intact shoot tissue (stems with leaves attached) and carefully placed into shallow plastic fresh cut herb containers (1 oz. hanging herb clamshell; goodstartpackaging, Bedford, NH). Postharvest sampling began once all destructive sampling was concluded during each harvest day (1400-1600 HR), as harvests later in the photoperiod may improve shelf-life compared with earlier harvests (Aharoni et al., 2010). The benefit of afternoon harvests could be a result of starch accumulation, which fluctuates in a diurnal fashion (Buchi et al., 1998). Plants with signs of mechanical damage or irregular blemishing were excluded from sampling to minimize confounding errors. Once

harvested, the herbs were promptly placed in two separate forced-air walk-in coolers (Thermo-kool walk-in cooler; Mid-south Industries, Laurel, MS) with AT setpoints of 10 or 4 °C. Temperature sensors (HOBO MX2301 temperature and relative humidity datalogger, Onset, Bourne, MA) measured and recorded cooler temperatures (ST °C). Basil 'Nufar' ST for reps 1, 2, and 3 for the for the 10 °C cooler were 10.2 ± 0.2 °C, 10.9 ± 1.1, and 10.4 ± 0.1 °C. The 10 °C cooler experienced malfunctions during each rep which dropped the temperature substantially below 10 °C; however, the timeline for basil 'Nufar' allowed us to complete the full 12 days of measurements, while the timeline for basil 'Red Rubin' forced us to use only the 4 °C cooler data. The 4 °C cooler datalogger experienced a malfunction which resulted in loss of temperature data beyond rep 1, thus the rep 1 temperature of 4.3 ± 0. 3 °C was substituted for all of the analyses.

Experimental design and data analysis

Plants were weighed without opening their containers every other day for three weeks following each harvest. Only time intervals which remained consistent across all reps were included in the statistical analyses (Table 4). Furthermore, the 4 °C walk-in cooler experienced multiple failures, thus the data from reps 1 and 3 are truncated.

After recording the weight of the fresh herb tissue over a 12-day period (12 DS), we subtracted the weight of the plastic containers from each recorded weight to determine the plant mass, then calculated the percent weight loss ($\Delta W_{d(x)}\%$) at each time interval.

The postharvest portion of the design was a split-plot arrangement with the two cooler temperatures as the main plots and time as the sub-plot, with repeated measures given each sample was repeatedly weighed over the course of storage.

After computing the $\Delta W_{d(x)}\%$, we analyzed our data with a linear mixed effects regression protocol included in the "lme4" and "lmetest" packages for R v4.3.3 software (R© Core Team, Vienna, Austria) and produced contour plots using the "ggplot2" package.
The equation for the full linear mixed effect response model is as follows: $y = \beta_1 + \beta_2 \cdot AT + \beta_3 \cdot NST + \beta_4 \cdot DS + \beta_5 \cdot ST + \beta_6 \cdot AT^2 + \beta_7 \cdot NST^2 + \beta_8 \cdot DS^2 + \beta_9 \cdot ST^2 + \beta_{10} \cdot AT \cdot NST + \beta_{11} \cdot AT \cdot DS + \beta_{12} \cdot NST \cdot DS + \beta_{13} \cdot AT \cdot ST + \beta_{14} \cdot NST \cdot ST + \beta_{15} \cdot DS \cdot ST + \beta_{16} \cdot AT \cdot NST \cdot DS + \beta_{17} \cdot AT \cdot NST \cdot ST + \beta_{18} \cdot AT \cdot DS \cdot ST + \beta_{19} \cdot NST \cdot DS \cdot ST + \beta_{20} \cdot AT \cdot NST \cdot DS \cdot ST$

Where β_1- β_{20} represent calculated model terms for the linear mixed effect responses, AT is air temperature, NST is nutrient solution temperature, DS is days of storage, and ST is storage temperature.

Results

All the percent weight loss values described henceforth are parameter estimates calculated via substation of the values in Table 4 for the corresponding model terms in the linear mixed effect regression equation provided on page 57 Those percent values represent the direct difference in percent weight loss between treatment combinations, rather than the magnitude of the difference. For instance, if plants grown in 20 °C AT and 15 °C NST lost 5% of their fresh weight after 4 days of storage in 10 C, whereas those grown in 20 °C AT with 20 °C NST lost 6% in the same storage condition, the difference would be reported as 1% greater in 20 °C AT with 20 °C NST.

Basil 'Nufar'

Air temperature, nutrient solution temperature, time, but not storage temperature, interacted to influence the mass of basil 'Nufar' in cold storage (**Table 4, Fig. 13**). Plants lost the greatest amount of weight over the first 4 DS, after which weight loss remained steady, but at a lower level. Percent weight loss decreased quadratically as AT increased from 20 to 30 °C, linearly as NST increased from 15 to 35 °C, and quadratically as ST increased from 4 to 10 °C. At 4 DS in 4 °C and 10 °C, plants grown in 20 °C AT with 15 and 20 °C NST lost 0.99% and 0.43% more mass than those grown in 30 °C AT with 15 and 20 °C NST. However, those grown in 20 °C AT with 25, 30, and 35 °C NST lost 0.12%, 0.68%, and 1.23% less mass than those grown in 30 °C AT with 25, 30, and 35 °C NST. By 12 DS in 4 °C and 10 °C, plants grown in 20 °C AT with 15, 20, 25, and 30 °C NST lost 5.55%, 3.89%, 2.22% and 0.56% more mass than those grown in 30 °C AT with 15, 20, 25, and 30 °C NST; however, those grown in 20 °C AT with 35 °C NST lost 1.1% less mass than those grown in 30 °C AT with 35 °C NST. Mass decreased quadratically with increasing post-harvest temperature.

Basil 'Red Rubin'

Air temperature, nutrient solution temperature, and days of storage interacted to influence weight loss in basil 'Red Rubin' samples stored for 12 days (**Table 4, Fig. 14**). At 6 days of storage, plants grown in 20 °C AT with 15, 20 and 25 °C NST lost 0.81%, 0.42%, and 0.02% less mass than those grown in 30 °C AT with 15, 20 and 25 °C NST. However, those grown in

Table 4. Basil 'Nufar' and 'Red Rubin' [Z]weight loss (% w/w) during storage. [Y]Model terms corresponding to linear mixed effect model on page 53 and [X]ns = response was not statistically significant.

	Basil'Nufar'	Basil 'Red Rubin'
Coefficient	Weight loss[Z] (% w/w)	Weight loss (% w/w)
β_1[Y]	-1.51E+02	-8.01E+01
β_2	1.69E+01	6.42E
β_3	9.70E-03	-7.68E-02
β_4	-4.09	ns
β_5	-1.68E+01	-1.50E+00
β_6	-3.41E-01	-1.33E-01
β_7	ns[X]	ns
β_8	3.67E-02	-4.31E-02
β_9	9.98E-01	ns
β_{10}	ns	7.24E-02
β_{11}	9.86E-02	3.32E-02
β_{12}	7.24E-02	ns
β_{13}	ns	ns
β_{14}	ns	ns
β_{15}	ns	ns
β_{16}	-2.77E-03	-1.32E-03
β_{17}	ns	ns
β_{18}	ns	ns
β_{19}	ns	ns
β_{20}	ns	ns

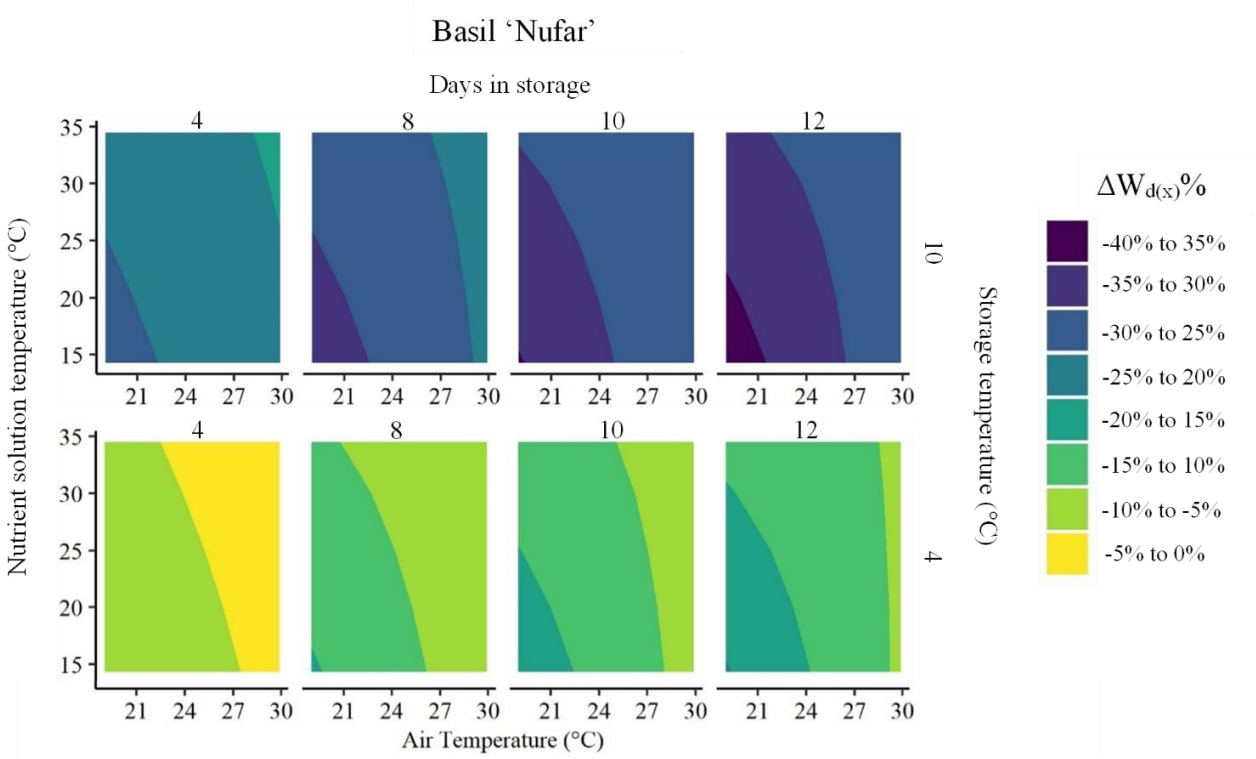


Figure 13. Air and nutrient solution temperature effects on weight loss during storage of basil (*Ocimum basilicum)* 'Nufar' over 4 to 12 days of storage in 4 or 10 °C.

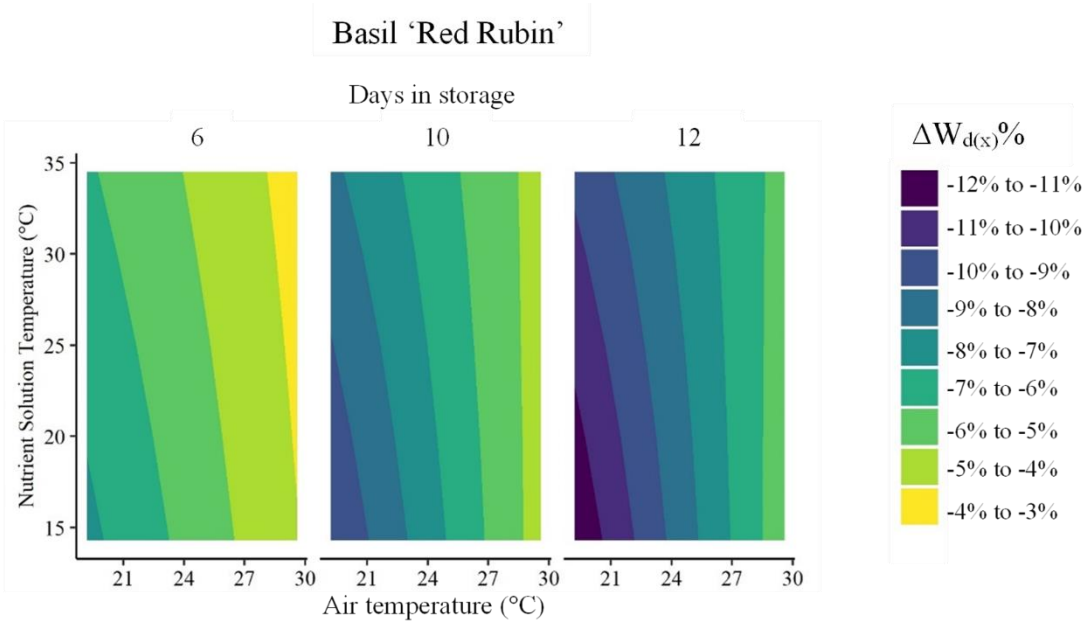


Figure 14. Air and nutrient solution temperature effects on weight loss during storage of basil (*Ocimum basilicum)* 'Red Rubin' over 6 to 12 days of storage.

20 °C AT with 30 and 35 °C NST lost 0.37% and 0.76% more mass than those grown in 30 °C AT with 30 and 35 °C NST. At 12 days of storage, plants grown in 20 °C AT lost more mass than those grown in 30 °C across all nutrient solution temperatures. Plants grown in 20 °C AT with 15, 20, 25, 30, and 35 °C NST lost 3.97%, 3.18%, 2.39%, 1.61%, and 0.82% more mass than those grown in 30 °C AT with 15, 20, 25, 30, and 35 °C NST.

Discussion

Air temperature, nutrient solution temperature, and time in storage, but not storage temperature interacted to influence the percentage of mass loss in basil 'Nufar' and 'Red Rubin' stored in 4 and 10 °C forced-air, walk-in coolers for a period of 12 days.

At 12 days of storage in 4 and 10 °C coolers, basil 'Nufar' grown in 15, 20, 25, and 30 °C NST with 30 °C AT, and basil 'Red Rubin' grown in 15, 20, 25, 30, and 35 °C NST with 30 °C AT, all lost less mass than those grown in the same NSTs with 20 °C AT. López-Blancas et al. (2014) found that basil 'Nufar' stored in 10 °C for 12 days lost roughly 10% of its fresh mass while those stored in 5 °C lost 6%, which corresponds to our basil 'Red Rubin' data, though basil 'Nufar' lost mass at roughly double that rate. The leaf to stem dry mass ratios (LSR) and node numbers (NN) (Chapter 2) could provide rough insight regarding the weight loss discrepancy between cultivars and treatment combinations. Basil 'Nufar' LSR was highest in plants grown in 20 °C AT with 15 °C NST (8.4 g leaf tissue per g stem tissue), while NN was highest in 30 °C AT with 30 °C NST (3.2); on the other hand Basil 'Red Rubin' LSR only responded to AT, and the highest was in 20 °C AT (4.4 g leaf tissue per g stem tissue), while NN responded to AT and NST but not their interaction, and was highest in 30 °C AT (4.5) or 25 °C NST (4.7). While we did not record leaf area, the LSR and NN provide indirect insight into a plant's morphology, as leaves produced by plants with higher LSRs and lower NNs (basil 'Nufar) were likely larger than those produced by plants with lower LSRs and higher NNs (basil 'Red Rubin'). We may reasonably assume the leaves were larger for the following reasons: LSR directly relates leaf weight to stem weight, and higher numbers mean leaves weighed more, and basil leaves are oppositely arranged (two per node). Thus, if basil 'Red Rubin' produced more nodes but lower LSRs, it produced more leaves which weighed less relative to their total mass. Plant leaves are the shoot organs which generally lose water at the greatest rate due to their high surface area and abundance of stomata on the adaxial and abaxial surfaces. Further, leaf tissues store large amounts of water to meet photosynthetic demand, regulate leaf temperature, expand tissues, and

provide structure. Basil stem tissue, on the other hand, possesses a much lower surface area with compactly arranged epidermal cells, and is less permeable to water. Thus basil 'Red Rubin', which had lower LSRs, had larger proportions of their overall weights comprised of stems, which may lose water at a slower rate than the leaves. Though LSR and NN are imperfect and indirect bases for comparing the species, the trend was conserved within species as well. Basil 'Nufar' LSR declined as AT and NST increased, and Basil 'Red Rubin' LSR decreased as AT increased. Likewise, as pre-harvest AT and NST increased, both cultivars lost less water in storage. While we may not positively state that LSR is causally linked to the water loss rate, it was correlated to some degree and a possible explanation for the trend. Aharoni et al. (2010) exposed basil to 38 °C for 8 h directly after harvest and found that CI incidence in 9 °C storage was reduced compared to those with no heat treatment which were stored in 9 °C, and suggested that heat shock proteins, higher antioxidant content, or a fungistatic effect could have been responsible. Though we used lower temperatures, basil grown in higher NSTs and ATs lost weight at a slower rate compared to those grown in lower NSTs and ATs.

Lange and Cameron (1997) grew basil in 24/20 °C day/night AT, and reported extremely short shelf-lives of 4 days maximum basil when was stored in 5 °C, but a doubling of the shelf-life when provided a 10 °C exposure for 4 h daily two days before harvest. Further, a full 24-h dark period at 10 °C prior to storage at 5 °C extended the shelf-life to ≈8 d. Larsen et al. (2023) grew basil in 15 and 25 °C AT, and found no difference in the development of CI in 4 or 12 °C storage; those grown in 15 °C AT were of poorer visual quality at harvest and had accumulated more soluble sugars, which could have allowed the plants to minimize water loss and maintain cellular functions. In our study, the difference in weight loss between plants grown in 25 and 15 °C NST was only marginal, which roughly aligns with their work.

In our study, plants grown in lower AT and NST produced higher dry matter concentrations than those grown in higher AT and NST (Ch. 2). If plants grown in higher AT and NST have greater water contents at harvest, the lower weight loss we observed over time could be due to those plants accumulating greater osmolyte concentrations, such as soluble sugars, thus allowing them to retain water for longer in storage.

Conclusion

Plants grown with higher air and nutrient solution temperatures lost water at a slower rate than those grown in lower temperature. Thus, for basil cultivars, nutrient solutions temperatures

around 25 to 30 °C achieve in 30 °C AT strike the ideal balance between storage longevity and fresh mass yield.

Literature cited

Abrami, G. (1972). Optimum mean temperature for a plant growth calculated by a new method of summation. *Ecology*, *53*(5), 893–900. https://doi.org/10.2307/1934305

Adhikari, L., Baral, R., Paudel, D., Min, D., Makaju, S. O., Poudel, H. P., Acharya, J. P., & Missaoui, A. M. (2022). Cold stress in plants: Strategies to improve cold tolerance in forage species. *Plant Stress*, *4*, 100081. https://doi.org/10.1016/j.stress.2022.100081

Aguilar-Santana, J. L., Jarimi, H., Velasco-Carrasco, M., & Riffat, S. (2020). Review on window-glazing technologies and future prospects. *International Journal of Low-Carbon Technologies*, *15*(1), 112–120. https://doi.org/10.1093/ijlct/ctz032

Aharoni, N., Kenigsbuch, D., Chalupowicz, D., Faura-Mlinski, M., Aharon, Z., Maurer, D., Ovadia, A., & Lers, A. (2010). Reducing chilling injury and decay in stored sweet basil. *Israel Journal of Plant Sciences, 58*, 167-181.

Ahemd, H. A., Al-Faraj, A. A., & Abdel-Ghany, A. M. (2016). Shading greenhouses to improve the microclimate, energy and water saving in hot regions: A review. *Scientia Horticulturae*, *201*, 36–45. https://doi.org/10.1016/j.scienta.2016.01.030

Akpenpuun, T. D., Ogunlowo, Q. O., Na, W.-H., Rabiu, A., Adesanya, M. A., Dutta, P., Zakir, E., Ogundele, O. M., Kim, H.-T., & Lee, H.-W. (2023). Review of temperature management strategies and techniques in the greenhouse microenvironment. *Adeleke University Journal of Engineering and Technology*, *6*(2), 126–147. http://aujet.adelekeuniversity.edu.ng/index.php/aujet/article/view/338

Al-Huqail, A., El-Dakak, R. M., Sanad, M. N., Badr, R. H., Ibrahim, M. M., Soliman, D., & Khan, F. (2020a). Effects of climate temperature and water stress on plant growth and accumulation of antioxidant compounds in sweet basil (*ocimum basilicum* l.) leafy vegetable. *Scientifica*, *2020*, 1–12. https://doi.org/10.1155/2020/3808909

Al-Huqail, A., El-Dakak, R. M., Sanad, M. N., Badr, R. H., Ibrahim, M. M., Soliman, D., & Khan, F. (2020b). Effects of climate temperature and water stress on plant growth and accumulation of antioxidant compounds in sweet basil (*ocimum basilicum* l.) leafy vegetable. *Scientifica, 2020*, 1–12. https://doi.org/10.1155/2020/3808909

Al-Mahdouri, A., Baneshi, M., Gonome, H., Okajima, J., & Maruyama, S. (2013). Evaluation of optical properties and thermal performances of different greenhouse covering materials. *Solar Energy*, *96*, 21–32. https://doi.org/10.1016/j.solener.2013.06.029

Alvarez, M. A. (2014). *Plant biotechnology for health: From secondary metabolites to molecular farming*. Springer International Publishing. https://doi.org/10.1007/978-3-319-05771-2

Ambroise, V., Legay, S., Guerriero, G., Hausman, J.-F., Cuypers, A., & Sergeant, K. (2020). The roots of plant frost hardiness and tolerance. *Plant and Cell Physiology*, *61*(1), 3–20. https://doi.org/10.1093/pcp/pcz196

Anyamba, A., Tucker, C. J., & Mahoney, R. (2002). From el niño to la niña: Vegetation response patterns over east and southern africa during the 1997–2000 period. *Journal of Climate*, *15*(21), 3096–3103. https://doi.org/10.1175/1520-0442(2002)015<3096:FENOTL>2.0.CO;2

Aquilanti, V., Mundim, K. C., Elango, M., Kleijn, S., & Kasai, T. (2010). Temperature dependence of chemical and biophysical rate processes: Phenomenological approach to deviations from Arrhenius law. *Chemical Physics Letters*, *498*(1–3), 209–213. https://doi.org/10.1016/j.cplett.2010.08.035

Ashraf, M. (2021). Thermotolerance in plants: Potential physio-biochemical and molecular markers for crop improvement. *Environmental and Experimental Botany*, *186*, 104454. https://doi.org/10.1016/j.envexpbot.2021.104454

Asseng, S., Ewert, F., Martre, P., Rötter, R. P., Lobell, D. B., Cammarano, D., Kimball, B. A., Ottman, M. J., Wall, G. W., White, J. W., Reynolds, M. P., Alderman, P. D., Prasad, P. V. V., Aggarwal, P. K., Anothai, J., Basso, B., Biernath, C., Challinor, A. J., De Sanctis, G., … Zhu, Y. (2015). Rising temperatures reduce global wheat production. *Nature Climate Change*, *5*(2), 143–147. https://doi.org/10.1038/nclimate2470

Atkin, O. K., & Tjoelker, M. G. (2003). Thermal acclimation and the dynamic response of plant respiration to temperature. *Trends in Plant Science*, *8*(7), 343–351. https://doi.org/10.1016/S1360-1385(03)00136-5

Badji, A., Benseddik, A., Bensaha, H., Boukhelifa, A., & Hasrane, I. (2022). Design, technology, and management of greenhouse: A review. *Journal of Cleaner Production*, *373*, 133753. https://doi.org/10.1016/j.jclepro.2022.133753

Balling, R. C., & Cerveny, R. S. (2003). Vertical dimensions of seasonal trends in the diurnal temperature range across the central United States. *Geophysical Research Letters*, *30*(17), 2003GL017776. https://doi.org/10.1029/2003GL017776

Barickman, T. C., Olorunwa, O. J., Sehgal, A., Walne, C. H., Reddy, K. R., & Gao, W. (2021). Interactive impacts of temperature and elevated co2 on basil (Ocimum basilicum L.) root and shoot morphology and growth. *Horticulturae*, *7*(5), 112. https://doi.org/10.3390/horticulturae7050112

Bartok, J. W. & Natural Resource, Agriculture, and Engineering Service (Eds.). (2001). *Energy conservation for commercial greenhouses* (2001 rev). Natural Resource, Agriculture, and Engineering Service.

Bastien, D., & Athienitis, A. K. (2017). Passive thermal energy storage, part 2: Design methodology for solaria and greenhouses. *Renewable Energy*, *103*, 537–560. https://doi.org/10.1016/j.renene.2016.11.041

Baumann, K. (2017). Membrane-to-nucleus signals modulate plant cold tolerance. *Nature Reviews Molecular Cell Biology*, *18*(5), 277–277. https://doi.org/10.1038/nrm.2017.38

Bergstrand, K.-J. I. (2017). Methods for growth regulation of greenhouse produced ornamental pot- and bedding plants – a current review. *Folia Horticulturae*, *29*(1), 63–74. https://doi.org/10.1515/fhort-2017-0007

Bredenbeck, H. (1985). Influence of different glazing materials on the light transmissivity of greenhouses. *Acta Horticulturae*, *170*, 111–118. https://doi.org/10.17660/ActaHortic.1985.170.12

Castro, R. P., Dinho Da Silva, P., & Pires, L. C. C. (2024). Advances in solutions to improve the energy performance of agricultural greenhouses: A comprehensive review. *Applied Sciences*, *14*(14), 6158. https://doi.org/10.3390/app14146158

Castroverde, C. D. M., & Dina, D. (2021). Temperature regulation of plant hormone signaling during stress and development. *Journal of Experimental Botany*, erab257. https://doi.org/10.1093/jxb/erab257

Chapman, J. M., Muhlemann, J. K., Gayomba, S. R., & Muday, G. K. (2019). Rboh-dependent ros synthesis and ros scavenging by plant specialized metabolites to modulate plant development and stress responses. *Chemical Research in Toxicology*, *32*(3), 370–396. https://doi.org/10.1021/acs.chemrestox.9b00028

Chau, J., Sowlati, T., Sokhansanj, S., Preto, F., Melin, S., & Bi, X. (2009). Techno-economic analysis of wood biomass boilers for the greenhouse industry. *Applied Energy*, *86*(3), 364–371. https://doi.org/10.1016/j.apenergy.2008.05.010

Copley, S. D. (2012). Toward a systems biology perspective on enzyme evolution. *Journal of Biological Chemistry*, *287*(1), 3–10. https://doi.org/10.1074/jbc.R111.254714
Cserháti, T. (2010). *Chromatography of aroma compounds and fragrances*. Springer.
Dusenge, M. E., Duarte, A. G., & Way, D. A. (2019). Plant carbon metabolism and climate change: Elevated CO_2 and temperature impacts on photosynthesis, photorespiration and respiration. *New Phytologist*, *221*(1), 32–49. https://doi.org/10.1111/nph.15283
Elings, A., Kempkes, F. L. K., Kaarsemaker, R. C., Ruijs, M. N. A., Van De Braak, N. J., & Dueck, T. A. (2005). The energy balance and energy-saving measures in greenhouse tomato cultivation. *Acta Horticulturae*, *691*, 67–74. https://doi.org/10.17660/ActaHortic.2005.691.5
Esteban, R., Olano, J. M., Castresana, J., Fernández-Marín, B., Hernández, A., Becerril, J. M., & García-Plazaola, J. I. (2009). Distribution and evolutionary trends of photoprotective isoprenoids (Xanthophylls and tocopherols) within the plant kingdom. *Physiologia Plantarum*, *135*(4), 379–389. https://doi.org/10.1111/j.1399-3054.2008.01196.x
Fallahi, H.-R., Mohammadi, M., Aghhavani-Shajari, M., & Ranjbar, F. (2015a). Determination of germination cardinal temperatures in two basil (Ocimum basilicum L.) cultivars using non-linear regression models. *Journal of Applied Research on Medicinal and Aromatic Plants*, *2*(4), 140–145. https://doi.org/10.1016/j.jarmap.2015.09.004
Fallahi, H.-R., Mohammadi, M., Aghhavani-Shajari, M., & Ranjbar, F. (2015b). Determination of germination cardinal temperatures in two basil (Ocimum basilicum L.) cultivars using non-linear regression models. *Journal of Applied Research on Medicinal and Aromatic Plants*, *2*(4), 140–145. https://doi.org/10.1016/j.jarmap.2015.09.004
Fonseca De Lima, C. F., Kleine-Vehn, J., De Smet, I., & Feraru, E. (2021). Getting to the root of belowground high temperature responses in plants. *Journal of Experimental Botany*, erab202. https://doi.org/10.1093/jxb/erab202
Foyer, C. H., & Hanke, G. (2022). ROS production and signalling in chloroplasts: Cornerstones and evolving concepts. *The Plant Journal*, *111*(3), 642–661. https://doi.org/10.1111/tpj.15856
Foyer, C. H., Lopez-Delgado, H., Dat, J. F., & Scott, I. M. (1997). Hydrogen peroxide- and glutathione-associated mechanisms of acclimatory stress tolerance and signalling. *Physiologia Plantarum*, *100*(2), 241–254. https://doi.org/10.1111/j.1399-3054.1997.tb04780.x

Frąszczak, B., & Knaflewski, M. (2009). Effect of light conditions and temperature on fresh yield of some spice plants grown in containers. *Journal of Fruit and Ornamental Plant Research*, *71*(1), 59–67. https://doi.org/10.2478/v10032-009-0027-6

Fratianni, F., Cefola, M., Pace, B., Cozzolino, R., De Giulio, B., Cozzolino, A., d'Acierno, A., Coppola, R., Logrieco, A. F., & Nazzaro, F. (2017). Changes in visual quality, physiological and biochemical parameters assessed during the postharvest storage at chilling or non-chilling temperatures of three sweet basil (Ocimum basilicum L.) cultivars. *Food Chemistry*, *229*, 752–760. https://doi.org/10.1016/j.foodchem.2017.02.137

Gabor, G., Stockinger, E. J., Francia, E., Milc, J., Kocsy, G., & Pecchioni, N. (2013). Freezing tolerance in the triticeae. In R. K. Varshney & R. Tuberosa (Eds.), *Translational Genomics for Crop Breeding* (1st ed., pp. 99–124). Wiley. https://doi.org/10.1002/9781118728482.ch7

Garcia, J. L., De La Plaza, S., Navas, L. M., Benavente, R. M., Luna, L., & Durán, J. M. (1998). Energy modelling for heated concrete floors in greenhouses. *Acta Horticulturae*, *456*, 355–362. https://doi.org/10.17660/ActaHortic.1998.456.42

Gasperi, D. (2017). *Urban horticulture: Reducing food miles to improve cities microclimate and environmental sustainability*. https://doi.org/10.6092/UNIBO/AMSDOTTORATO/8022

Ghorbani, A., & Esmaeilizadeh, M. (2017). Pharmacological properties of Salvia officinalis and its components. *Journal of Traditional and Complementary Medicine*, *7*(4), 433–440. https://doi.org/10.1016/j.jtcme.2016.12.014

Golzar, F., Heeren, N., Hellweg, S., & Roshandel, R. (2018). A novel integrated framework to evaluate greenhouse energy demand and crop yield production. *Renewable and Sustainable Energy Reviews*, *96*, 487–501. https://doi.org/10.1016/j.rser.2018.06.046

Gote,G. N. and Padghan,P. R. (2009), 20093099946, English, Journal article, India, 0976-8947 0973-4759, 3, (2), Muzaffarnagar, Asian Journal of Environmental Science, (158–161), Hind Agri-Horticultural Society, Studies on different thermal regimes and thermal sensitivity analysis of tomato genotypes.

Guo, Y., Zhao, H., Zhang, S., Wang, Y., & Chow, D. (2021). Modeling and optimization of environment in agricultural greenhouses for improving cleaner and sustainable crop production. *Journal of Cleaner Production*, *285*, 124843. https://doi.org/10.1016/j.jclepro.2020.124843

Hao, X., Jewett, T., Zheng, J., & Khosla, S. (2005). Microclimate and energy consumption in commercial, hot-water and steam heated greenhouses for tomato production. *Acta Horticulturae*, *691*, 171–178. https://doi.org/10.17660/ActaHortic.2005.691.19

Harborne, J. B. (1999). Classes and functions of secondary products from plants. In N. J. Walton & D. E. Brown, *Chemicals from Plants* (pp. 1–25). WORLD SCIENTIFIC / IMPERIAL COLLEGE PRESS. https://doi.org/10.1142/9789812817273_0001

Hare, J. G., Norton, B., & Probert, S. D. (1984). Design of 'greenhouses': Thermal aspects. *Applied Energy*, *18*(1), 49–82. https://doi.org/10.1016/0306-2619(84)90045-X

Hasanuzzaman, M., Nahar, K., Alam, Md., Roychowdhury, R., & Fujita, M. (2013). Physiological, biochemical, and molecular mechanisms of heat stress tolerance in plants. *International Journal of Molecular Sciences*, *14*(5), 9643–9684. https://doi.org/10.3390/ijms14059643

Hassan, M. U., Chattha, M. U., Khan, I., Chattha, M. B., Barbanti, L., Aamer, M., Iqbal, M. M., Nawaz, M., Mahmood, A., Ali, A., & Aslam, M. T. (2021). Heat stress in cultivated plants: Nature, impact, mechanisms, and mitigation strategies—a review. *Plant Biosystems - An International Journal Dealing with All Aspects of Plant Biology*, *155*(2), 211–234. https://doi.org/10.1080/11263504.2020.1727987

Hatfield, J. L., Boote, K. J., Kimball, B. A., Ziska, L. H., Izaurralde, R. C., Ort, D., Thomson, A. M., & Wolfe, D. (2011). Climate impacts on agriculture: Implications for crop production. *Agronomy Journal*, *103*(2), 351–370. https://doi.org/10.2134/agronj2010.0303

He, F., Tian, J., Wang, L., Hou, Y., Qi, F., Zhang, Y., Zhu, L., Li, Z., 1 (2022). Academy of Agricultural Planning and Engineering, Ministry of Agriculture and Rural Affairs, Beijing 100125, China, 2. Key Laboratory of Farm Building in Structure and Intelligent Construction, Ministry of Agriculture and Rural Affairs, Beijing 100125, China, & 3. Hebei Agricultural University, Baoding 071001, Hebei, China. Effects of different root zone heating systems on the microclimate and crop development in solar greenhouses. *International Journal of Agricultural and Biological Engineering*, *15*(6), 67–72. https://doi.org/10.25165/j.ijabe.20221506.7581

Hendrickson, T., Dunn, B. L., Goad, C., Hu, B., & Singh, H. (2022). Effects of elevated water temperature on growth of basil using nutrient film technique. *HortScience*, *57*(8), 925–932. https://doi.org/10.21273/HORTSCI16690-22

Hepbasli, A. (2011). A comparative investigation of various greenhouse heating options using exergy analysis method. *Applied Energy*, *88*(12), 4411–4423. https://doi.org/10.1016/j.apenergy.2011.05.022

Hikosaka, K., Ishikawa, K., Borjigidai, A., Muller, O., & Onoda, Y. (2006). Temperature acclimation of photosynthesis: Mechanisms involved in the changes in temperature dependence of photosynthetic rate. *Journal of Experimental Botany*, *57*(2), 291–302. https://doi.org/10.1093/jxb/erj049

Hu, Y., Jiang, Y., Han, X., Wang, H., Pan, J., & Yu, D. (2017). Jasmonate regulates leaf senescence and tolerance to cold stress: Crosstalk with other phytohormones. *Journal of Experimental Botany*, *68*(6), 1361–1369. https://doi.org/10.1093/jxb/erx004

Hückstädt, A. B., Mortensen, L. M., & Gislerød, H. R. (2013). The effect of high maximum day temperatures and coloured film cover on growth and morphogenesis of some herbs in a CO2 enriched greenhouse atmosphere. *Eur. J. Hortic. Sci*, *78*(5), 203-208.

Hurewitz, J., & Janes, H. W. (1983). Effect of altering the root-zone temperature on growth, translocation, carbon exchange rate, and leaf starch accumulation in the tomato. *Plant Physiology*, *73*(1), 46–50. https://doi.org/10.1104/pp.73.1.46

Imler, C., Frantz, J. M., & Currey, C. J. (2022). Quantifying how diurnal temperature differences affect lettuce and basil under moderate and warm average daily temperatures. *2022 ASHS Annual Conference*. https://ashs.confex.com/ashs/2022/meetingapp.cgi/Paper/38371

Inthichack, P., Nishimura, Y., & Fukumoto, Y. (2013). Diurnal temperature alternations on plant growth and mineral absorption in eggplant, sweet pepper, and tomato. *Horticulture, Environment, and Biotechnology*, *54*(1), 37–43. https://doi.org/10.1007/s13580-013-0106-y

Islam, N., Torre, S., Wold, A. B., & GislerØd, H. R. (2016). Effect of temperature DIF and drop on the growth, quality, total phenolic content and antioxidant activity of herbs. J. Multidiscip. Eng. Sci. Stud, 2, 266-271.

Kamatchi, K.A.M., Anitha, K., Kumar, K.A. *et al.* Impacts of combined drought and high-temperature stress on growth, physiology, and yield of crops. *Plant Physiol. Rep.* **29**, 28–36 (2024). https://doi.org/10.1007/s40502-023-00754-4

Kawasaki, Y., & Yoneda, Y. (2019). Local temperature control in greenhouse vegetable production. *The Horticulture Journal*, *88*(3), 305–314. https://doi.org/10.2503/hortj.UTD-R004

Kestin, J., Sengers, J. V., Kamgar-Parsi, B., & Sengers, J. M. H. L. (1984). Thermophysical properties of fluid h2o. *Journal of Physical and Chemical Reference Data*, *13*(1), 175–183. https://doi.org/10.1063/1.555707

Kim, H.-Y., Yu, O.-Y., & Ferrell, J. (2024). Case study: Reducing heating energy consumption in a high tunnel greenhouse with renewable energy and microclimate control by bench-top root-zone heating, bench covers, and under-bench insulation. *Discover Sustainability*, *5*(1), 86. https://doi.org/10.1007/s43621-024-00276-5

Kläring, H.-P., Klopotek, Y., Krumbein, A., & Schwarz, D. (2015). The effect of reducing the heating set point on the photosynthesis, growth, yield and fruit quality in greenhouse tomato production. *Agricultural and Forest Meteorology*, *214–215*, 178–188. https://doi.org/10.1016/j.agrformet.2015.08.250

Lange, D. D., & Cameron, A. C. (1994). Postharvest Shelf Life of Sweet Basil (Ocimum basilicum). *HortScience HortSci*, *29*(2), 102-103., https://doi.org/10.21273/HORTSCI.29.2.102

Lange, D. L., & Camero, A. C. (1997). Pre- and Postharvest Temperature Conditioning of Greenhouse-grown Sweet Basil. *HortScience HortSci*, *32*(1), 114-116., https://doi.org/10.21273/HORTSCI.32.1.114

Larsen, D. H., Marcelis, L. F. M., Van Kempen, D., Kohlen, W., Nicole, C. C. S., & Woltering, E. J. (2023). Far-red light during cultivation improves postharvest chilling tolerance in basil. *Postharvest Biology and Technology*, *198*, 112232., https://doi.org/10.1016/j.postharvbio.2022.112232

Li, C., Kong, X., Luo, Z., Li, W., Tang, W., Zhang, D., Ma, C., & Dong, H. (2021). Exogenous application of acetic acid improves the survival rate of cotton by increasing abscisic acid and jasmonic acid contents under drought stress. *Acta Physiologiae Plantarum*, *43*(2), 32. https://doi.org/10.1007/s11738-021-03202-8

Li, G., Tang, L., Zhang, X., Dong, J., & Xiao, M. (2018). Factors affecting greenhouse microclimate and its regulating techniques: A review. *IOP Conference Series: Earth and Environmental Science*, *167*, 012019. https://doi.org/10.1088/1755-1315/167/1/012019

Li, J., Martin, A., Carver, L., Armstrong, S., Givens, S., & Walters, K. (2024). Optimizing sowing density for parsley, cilantro, and sage in controlled environment production: Balancing productivity and plant quality. *HortTechnology*, *34*(3), 305–312. https://doi.org/10.21273/HORTTECH05381-23

Li, Z., Ma, X., Zhao, Y., & Zheng, H. (2019). Study on the performance of a curved fresnel solar concentrated system with seasonal underground heat storage for the greenhouse application. *Journal of Solar Energy Engineering, 141*(1), 011004. https://doi.org/10.1115/1.4040839

Lichtenthaler, H. K. (1996). Vegetation stress: An introduction to the stress concept in plants. *Journal of Plant Physiology, 148*(1–2), 4–14. https://doi.org/10.1016/S0176-1617(96)80287-2

Lorenzo, P., Reyes, R., Medrano, E., Granados, R., Bonachela, S., Hernández, J., López, J. C., Magán, J. J., Del Amor, F. M., & Sánchez-Guerrero, M. C. (2024). Hybrid passive cooling and heating system for Mediterranean greenhouses. Microclimate and sweet pepper crop response. *Agricultural Water Management, 301*, 108937. https://doi.org/10.1016/j.agwat.2024.108937

Luo, Q. (2011). Temperature thresholds and crop production: A review. *Climatic Change, 109*(3–4), 583–598. https://doi.org/10.1007/s10584-011-0028-6

Lynch, J., Marschner, P., & Rengel, Z. (2012). Effect of internal and external factors on root growth and development. In *Marschner's Mineral Nutrition of Higher Plants* (pp. 331–346). Elsevier. https://doi.org/10.1016/B978-0-12-384905-2.00013-3

Maeda, H. A. (2019). Evolutionary diversification of primary metabolism and its contribution to plant chemical diversity. *Frontiers in Plant Science, 10*. https://www.frontiersin.org/articles/10.3389/fpls.2019.00881

Mahan, J. (1995). Methods for reducing the adverse effects of temperature stress on plants: A review. *Environmental and Experimental Botany, 35*(3), 251–258. https://doi.org/10.1016/0098-8472(95)00011-6

Mata, D. A., & Botto, J. F. (2011). Photoperiod, light, and temperature requirements to control plant architecture and flowering time in *Salvia exserta*. *The Journal of Horticultural Science and Biotechnology*, *86*(4), 408–414. https://doi.org/10.1080/14620316.2011.11512782

Maxwell, K., & Johnson, G. N. (2000). Chlorophyll fluorescence—A practical guide. *Journal of Experimental Botany*, *51*(345), 659–668. https://doi.org/10.1093/jexbot/51.345.659

McCartney, L., & Lefsrud, M. (2018). Protected agriculture in extreme environments: A review of controlled environment agriculture in tropical, arid, polar, and urban locations. *Applied Engineering in Agriculture, 34*(2), 455–473. https://doi.org/10.13031/aea.12590

Michaletz, S. T., Weiser, M. D., Zhou, J., Kaspari, M., Helliker, B. R., & Enquist, B. J. (2015). Plant thermoregulation: Energetics, trait–environment interactions, and carbon economics. *Trends in Ecology & Evolution, 30*(12), 714–724. https://doi.org/10.1016/j.tree.2015.09.006

Miller, A., Langenhoven, P., & Nemali, K. (2020). Maximizing productivity of greenhouse-grown hydroponic lettuce during winter. *HortScience, 55*(12), 1963–1969. https://doi.org/10.21273/HORTSCI15351-20

Moon, J. H., Kang, Y. K., & Suh, H. D. (2007). Effect of root-zone cooling on the growth and yield of cucumber at supraoptimal air temperature. *Acta Horticulturae, 761,* 271–274. https://doi.org/10.17660/ActaHortic.2007.761.36

Mortensen, L. M. (2014). The effect of air temperature on growth of eight herb species. *American Journal of Plant Sciences, 5*(11), 1542–1546. https://doi.org/10.4236/ajps.2014.511168

Mueller, S. P., Unger, M., Guender, L., Fekete, A., & Mueller, M. J. (2017). Phospholipid:diacylglycerol acyltransferase-mediated triacylglyerol synthesis augments basal thermotolerance. *Plant Physiology, 175*(1), 486–497. https://doi.org/10.1104/pp.17.00861

Mundim, K. C., Baraldi, S., Machado, H. G., & Vieira, F. M. C. (2020). Temperature coefficient (Q10) and its applications in biological systems: Beyond the Arrhenius theory. *Ecological Modelling, 431,* 109127. https://doi.org/10.1016/j.ecolmodel.2020.109127

Mundler, P., & Rumpus, L. (2012). The energy efficiency of local food systems: A comparison between different modes of distribution. *Food Policy, 37*(6), 609–615. https://doi.org/10.1016/j.foodpol.2012.07.006

Naing, A. H., & Kim, C. K. (2021). Abiotic stress-induced anthocyanins in plants: Their role in tolerance to abiotic stresses. *Physiologia Plantarum, 172*(3), 1711–1723. https://doi.org/10.1111/ppl.13373

Nguyen, D. T. P., Lu, N., Kagawa, N., Kitayama, M., & Takagaki, M. (2020). Short-term root-zone temperature treatment enhanced the accumulation of secondary metabolites of hydroponic coriander (Coriandrum sativum L.) grown in a plant factory. *Agronomy, 10*(3), 413. https://doi.org/10.3390/agronomy10030413

Nguyen, D. T. P., Lu, N., Kagawa, N., & Takagaki, M. (2019). Optimization of photosynthetic photon flux density and root-zone temperature for enhancing secondary metabolite accumulation and production of coriander in plant factory. *Agronomy, 9*(5), 224. https://doi.org/10.3390/agronomy9050224

Nguyen, L., Duong, L. T., & Mentreddy, R. S. (2019). The U.S. import demand for spices and herbs by differentiated sources. *Journal of Applied Research on Medicinal and Aromatic Plants*, *12*, 13–20. https://doi.org/10.1016/j.jarmap.2018.12.001

Nkansah, G. O., & Ito, T. (1994). Comparative studies on growth and development of heat-tolerant and non heat-tolerant tomato plants grown at different root-zone temperatures. *Engei Gakkai Zasshi*, *62*(4), 775–780. https://doi.org/10.2503/jjshs.62.775

Obata, T. (2019). Metabolons in plant primary and secondary metabolism. *Phytochemistry Reviews*, *18*(6), 1483–1507. https://doi.org/10.1007/s11101-019-09619-x

Öquist, G. (1983). Effects of low temperature on photosynthesis. *Plant, Cell & Environment*, *6*(4), 281–300. https://doi.org/10.1111/1365-3040.ep11612087

Örvar, B. L., Sangwan, V., Omann, F., & Dhindsa, R. S. (2000). Early steps in cold sensing by plant cells: The role of actin cytoskeleton and membrane fluidity. *The Plant Journal*, *23*(6), 785–794. https://doi.org/10.1046/j.1365-313x.2000.00845.x

Penfield, S. (2008). Temperature perception and signal transduction in plants. *New Phytologist*, *179*(3), 615–628. https://doi.org/10.1111/j.1469-8137.2008.02478.x

Peraudeau, S., Lafarge, T., Roques, S., Quiñones, C. O., Clement-Vidal, A., Ouwerkerk, P. B. F., Van Rie, J., Fabre, D., Jagadish, K. S. V., & Dingkuhn, M. (2015). Effect of carbohydrates and night temperature on night respiration in rice. *Journal of Experimental Botany*, *66*(13), 3931–3944. https://doi.org/10.1093/jxb/erv193

Pichersky, E., & Gang, D. R. (2000). Genetics and biochemistry of secondary metabolites in plants: An evolutionary perspective. *Trends in Plant Science*, *5*(10), 439–445. https://doi.org/10.1016/S1360-1385(00)01741-6

Poelwijk, F. J., Kiviet, D. J., Weinreich, D. M., & Tans, S. J. (2007). Empirical fitness landscapes reveal accessible evolutionary paths. *Nature*, *445*(7126), 383–386. https://doi.org/10.1038/nature05451

Pospíšil, P., & Prasad, A. (2014). Formation of singlet oxygen and protection against its oxidative damage in Photosystem II under abiotic stress. *Journal of Photochemistry and Photobiology B: Biology*, *137*, 39–48. https://doi.org/10.1016/j.jphotobiol.2014.04.025

Pott, D. M., Osorio, S., & Vallarino, J. G. (2019). From central to specialized metabolism: An overview of some secondary compounds derived from the primary metabolism for their role in

conferring nutritional and organoleptic characteristics to fruit. *Frontiers in Plant Science*, *10*, 835. https://doi.org/10.3389/fpls.2019.00835

Prusinowska, R., & Śmigielski, K. (2015). Losses of essential oils and antioxidants during the drying of herbs and spices. A review. *Engineering Sciences And Technologies*, *2*. https://doi.org/10.15611/nit.2015.2.05

R Core Team (2021). R: A language and environment for statistical computing. R Foundation for Statistical Computing, Vienna, Austria. URL: https://www.R-project.org/.

Runkle, E., & Both, A. J. (2011). *Greenhouse energy conservation strategies*. https://doi.org/10.7282/T3K64KWN

Sage, T. L., Bagha, S., Lundsgaard-Nielsen, V., Branch, H. A., Sultmanis, S., & Sage, R. F. (2015). The effect of high temperature stress on male and female reproduction in plants. *Field Crops Research*, *182*, 30–42. https://doi.org/10.1016/j.fcr.2015.06.011

Sánchez, F. J., Manzanares, M., De Andres, E. F., Tenorio, J. L., & Ayerbe, L. (1998). Turgor maintenance, osmotic adjustment and soluble sugar and proline accumulation in 49 pea cultivars in response to water stress. *Field Crops Research*, *59*(3), 225–235. https://doi.org/10.1016/S0378-4290(98)00125-7

Seigler, D. S. (1998). *Plant secondary metabolism*. Springer US. https://doi.org/10.1007/978-1-4615-4913-0

Sethi, V. P., & Sharma, S. K. (2007). Survey of cooling technologies for worldwide agricultural greenhouse applications. *Solar Energy*, *81*(12), 1447–1459. https://doi.org/10.1016/j.solener.2007.03.004

Shamshiri, R. R., Jones, J. W., Thorp, K. R., Ahmad, D., Man, H. C., & Taheri, S. (2018). Review of optimum temperature, humidity, and vapour pressure deficit for microclimate evaluation and control in greenhouse cultivation of tomato: A review. *International Agrophysics*, *32*(2), 287–302. https://doi.org/10.1515/intag-2017-0005

Shen Xiaocheng, Lu Jiqi, Ren Yingdang, Shen Qi, You Zhixing, Liu Xintao, Zhang Shujie, Wang Guanghua, & Yang Linlin. (2022). Distribution pattern and geographical division of terrestrial living things in the world. *Journal of Environmental Science and Engineering B*, *11*(5). https://doi.org/10.17265/2162-5263/2022.05.002

Sigrimis, N., Anastasiou, A., & Rerras, N. (2000). Energy saving in greenhouses using temperature integration: A simulation survey. *Computers and Electronics in Agriculture*, *26*(3), 321–341. https://doi.org/10.1016/S0168-1699(00)00083-1

Silva, M. G. D., Soares, T. M., Gheyi, H. R., Santos, C. C. D., & Oliveira, M. G. B. D. (2022). Hydroponic cultivation of coriander intercropped with rocket subjected to saline and thermal stresses in the root-zone. *Revista Ceres*, *69*(2), 148–157. https://doi.org/10.1590/0034-737x202269020004

Slattery, R. A., & Ort, D. R. (2019). Carbon assimilation in crops at high temperatures. *Plant, Cell & Environment*, *42*(10), 2750–2758. https://doi.org/10.1111/pce.13572

Solis-Toapanta, E., Fisher, P., & Gómez, C. (2020). Growth rate and nutrient uptake of basil in small-scale hydroponics. *HortScience*, *55*(4), 507–514. https://doi.org/10.21273/HORTSCI14727-19

Spence, C. (2021). What is the relationship between the presence of volatile organic compounds in food and drink products and multisensory flavour perception? *Foods*, *10*(7), 1570. https://doi.org/10.3390/foods10071570

Stein, A.J., Santini, F. The sustainability of "local" food: a review for policy-makers. *Rev Agric Food Environ Stud* **103**, 77–89 (2022). https://doi.org/10.1007/s41130-021-00148-w.

Steward, Darlene M., & Avery, Greg (2022). Controlled-Environment Agriculture and the Geography of Food, Energy and Water Resilience in the United States.

Suzuki, N., Miller, G., Salazar, C., Mondal, H. A., Shulaev, E., Cortes, D. F., Shuman, J. L., Luo, X., Shah, J., Schlauch, K., Shulaev, V., & Mittler, R. (2013). Temporal-spatial interaction between reactive oxygen species and abscisic acid regulates rapid systemic acclimation in plants. *The Plant Cell*, *25*(9), 3553–3569. https://doi.org/10.1105/tpc.113.114595

Suzuki, N., & Mittler, R. (2006). Reactive oxygen species and temperature stresses: A delicate balance between signaling and destruction. *Physiologia Plantarum*, *126*(1), 45–51. https://doi.org/10.1111/j.0031-9317.2005.00582.x

Terrosi, C., Cacini, S., Burchi, G., Cutini, M., Brambilla, M., Bisaglia, C., Massa, D., & Fedrizzi, M. (2020). Evaluation of compressor heat pump for root zone heating as an alternative heating source for leafy vegetable cultivation. *Energies*, *13*(3), 745. https://doi.org/10.3390/en13030745

Thompson, H. C., Langhans, R. W., Both, A.-J., & Albright, L. D. (1998). Shoot and root temperature effects on lettuce growth in a floating hydroponic system. *Journal of the American Society for Horticultural Science*, *123*(3), 361–364. https://doi.org/10.21273/JASHS.123.3.361

Urone, P. P., & Hinrichs, R. (2020, March 26). *11. 2 heat, specific heat, and heat transfer—Physics | openstax*. https://openstax.org/books/physics/pages/11-2-heat-specific-heat-and-heat-transfer

Van Iersel, M. W. (2006). Respiratory Q $_{10}$ of marigold (*tagetes patula*) in response to long-term temperature differences and its relationship to growth and maintenance respiration. *Physiologia Plantarum*, *128*(2), 289–301. https://doi.org/10.1111/j.1399-3054.2006.00743.x

Van Passel, S. (2013). Food miles to assess sustainability: A revision. *Sustainable Development*, *21*(1), 1–17. https://doi.org/10.1002/sd.485

Vázquez-Hernández, M. C., Parola-Contreras, I., Montoya-Gómez, L. M., Torres-Pacheco, I., Schwarz, D., & Guevara-González, R. G. (2019). Eustressors: Chemical and physical stress factors used to enhance vegetables production. *Scientia Horticulturae*, *250*, 223–229. https://doi.org/10.1016/j.scienta.2019.02.053

Vitor, D. M., De Araujo, F. F., & Finger, F. L. (2018). Development of chilling injury in potted 'Genovese' sweet basil. *Acta Horticulturae*, *1194*, 451–456. https://doi.org/10.17660/ActaHortic.2018.1194.65

Waliczek, T. M., & Zajicek, J. M. (Eds.). (2016). *Urban horticulture*. CRC Press/Taylor & Francis Group.

Walters, K. J., & Currey, C. J. (2019). Growth and development of basil species in response to temperature. *HortScience*, *54*(11), 1915–1920. https://doi.org/10.21273/HORTSCI12976-18

Way, D. A., & Yamori, W. (2014). Thermal acclimation of photosynthesis: On the importance of adjusting our definitions and accounting for thermal acclimation of respiration. *Photosynthesis Research*, *119*(1–2), 89–100. https://doi.org/10.1007/s11120-013-9873-7

Willits, D. H., & Peet, M. M. (1998). The effect of night temperature on greenhouse grown tomato yields in warm climates. *Agricultural and Forest Meteorology*, *92*(3), 191–202. https://doi.org/10.1016/S0168-1923(98)00089-6

Wu, Y.-B., Ni, Z.-Y., Shi, Q.-W., Dong, M., Kiyota, H., Gu, Y.-C., & Cong, B. (2012). Constituents from *salvia* species and their biological activities. *Chemical Reviews*, *112*(11), 5967–6026. https://doi.org/10.1021/cr200058f

Yamori, W., Noguchi, K., & Terashima, I. (2005). Temperature acclimation of photosynthesis in spinach leaves: Analyses of photosynthetic components and temperature dependencies of photosynthetic partial reactions. *Plant, Cell & Environment*, *28*(4), 536–547. https://doi.org/10.1111/j.1365-3040.2004.01299.x

Yan, W. (1999). An equation for modelling the temperature response of plants using only the cardinal temperatures. *Annals of Botany*, *84*(5), 607–614. https://doi.org/10.1006/anbo.1999.0955

Yıldız, İ. (2021). *Greenhouse engineering: Integrated energy management* (1st ed.). CRC Press. https://doi.org/10.1201/9781315117072

Zhang, H., & Sonnewald, U. (2017). Differences and commonalities of plant responses to single and combined stresses. *The Plant Journal*, *90*(5), 839–855. https://doi.org/10.1111/tpj.13557

Zhang, X., Lv, J., Dawuda, M. M., Xie, J., Yu, J., Gan, Y., Zhang, J., Tang, Z., & Li, J. (2019). Innovative passive heat-storage walls improve thermal performance and energy efficiency in Chinese solar greenhouses for non-arable lands. *Solar Energy*, *190*, 561–575. https://doi.org/10.1016/j.solener.2019.08.056

Zhu, H., Zhang, T. J., Zheng, J., Huang, X. D., Yu, Z. C., Peng, C. L., & Chow, W. S. (2018). Anthocyanins function as a light attenuator to compensate for insufficient photoprotection mediated by nonphotochemical quenching in young leaves of Acmena acuminatissima in winter. *Photosynthetica*, *56*(SPECIAL ISSUE), 445–454. https://doi.org/10.1007/s11099-017-0740-1

---. “Thermophysical Properties of Fluid H2O.” *Journal of Physical and Chemical Reference Data*, vol. 13, no. 1, Jan. 1984, pp. 175–83. *DOI.org (Crossref)*, https://doi.org/10.1063/1.555707.

2016 ashs annual conference: Oral session-herbs, spices, and medicinal plants 2. (n.d.). Retrieved November 8, 2024, from https://ashs.confex.com/ashs/2016/webprogramarchives/Session8103.html

Vita

Spencer Givens is a Tennessee native who received his Bachelor of Science degree in plant science from the University of Tennessee, Knoxville in 2022. He initially worked in Dr. Kellie Walters' laboratory as an undergraduate research assistant, and after completing his degree he began his Master of Science program in the same laboratory.